





## Article

# Early Periods of Low-Temperature Linear Antenna CVD Nucleation and Growth Study of Nanocrystalline Diamond Films

Awadesh Kumar Mallik <sup>1,\*</sup>, Wen-Ching Shih <sup>1,2</sup>, Paulius Pobedinskas <sup>1</sup> and Ken Haenen <sup>1</sup>

<sup>1</sup> Institute for Materials Research (IMO), Hasselt University and IMOMEC, IMEC vzw, Wetenschapspark 1, 3590 Diepenbeek, Belgium; wcshih@ttu.edu.tw (W.-C.S.); paulius.pobedinskas@uhasselt.be (P.P.); ken.haenen@uhasselt.be (K.H.)

<sup>2</sup> Department of Electrical Engineering, Tatung University, Taipei 10451, Taiwan

\* Correspondence: awadesh.mallik@gmail.com or awadesh.mallik@ntu.edu.sg

† Currently address: Nanyang Technological University, Singapore 637553, Singapore.

**Abstract:** Low-temperature growth of diamond films using the chemical vapor deposition (CVD) method is not so widely reported and its initial periods of nucleation and growth phenomenon are of particular interest to the researchers. Four sets of substrates were selected for growing diamond films using linear antenna microwave plasma-enhanced CVD (LA-MPCVD). Among them, silicon and sapphire substrates were pre-treated with detonation nanodiamond (DND) seeds before diamond growth, for enhancement of its nucleation. Carbon nanotube (CNT) films on Si substrates were also used as another template for LA-MPCVD diamond growth. To enhance diamond nucleation during CVD growth, some of the CNT films were again pre-treated by the electrophoretic deposition (EPD) of diamond nanoparticles. All these substrates were then put inside the LA-MPCVD chamber to grow diamond films under variable processing conditions. Microwave input powers (1100–2800 W), input power modes (pulse or continuous), antenna-to-stage distances (5–6.5 cm), process gas recipes (with or without CO<sub>2</sub>), methane gas percentages (3%–5%), and deposition times (11–120 min) were altered to investigate their effect on the growth of diamond film on the pre-treated substrates. The substrate temperatures were found to vary from as low as 170 °C to a maximum of 307 °C during the alteration of the different processing parameters. Contrary to the conventional MPCVD, it was observed that during the first hour of LA-MPCVD diamond growth, DND seeds and the nucleating structures do not coalesce together to make a continuous film. Deposition time was the most critical factor in fully covering the substrate surfaces with diamond film, since the substrate temperature could not become stable during the first hour of LA-MPCVD. CNTs were found to be oxidized rapidly under LA-MPCVD plasma conditions; therefore, a CO<sub>2</sub>-free process gas recipe was used to reduce CNT burning. Moreover, EPD-coated CNTs were found to be less oxidized by the LACVD plasma during diamond growth.

**Keywords:** linear antenna microwave plasma chemical vapor deposition (LA-MPCVD); early growth stage; low temperature; nanodiamond; carbon nanotube (CNT); substrate seeding



**Citation:** Mallik, A.K.; Shih, W.-C.; Pobedinskas, P.; Haenen, K. Early Periods of Low-Temperature Linear Antenna CVD Nucleation and Growth Study of Nanocrystalline Diamond Films. *Coatings* **2024**, *14*, 184. <https://doi.org/10.3390/coatings14020184>

Academic Editors: Igor K. Igumenov and Vladimir Lukashov

Received: 21 December 2023

Revised: 19 January 2024

Accepted: 29 January 2024

Published: 31 January 2024



**Copyright:** © 2024 by the authors. Licensee MDPI, Basel, Switzerland. This article is an open access article distributed under the terms and conditions of the Creative Commons Attribution (CC BY) license (<https://creativecommons.org/licenses/by/4.0/>).

## 1. Introduction

CVD growth of diamond films occurs within the temperature range of 700–1100 °C [1]. There are also reports of growing diamond films at substrate temperatures of 500 °C or less [2–6]. Linear antenna microwave plasma-enhanced CVD (LA-MPCVD) is a process [7–13] that allows the growth of diamond crystals at lower substrate temperatures [14–16]. However, there is very little literature available in which growth has been reported at a temperature of less than 300 °C [17,18]. Reporting of the respective substrate temperature during CVD has mostly been carried out in situ, using optical pyrometers [19], but low LA-MPCVD processing temperatures do not allow the use of such optical instruments [15].

Therefore, thermocouples and infrared thermometers are placed underneath the substrate stage to reliably record the LA-MPCVD growth temperatures, where it is protected or uninfluenced from the effect of CVD plasma in the diamond growth environment. In this paper, experiments have been designed to allow diamond growth at less than 300 °C. It is also well known that during the first few minutes of CVD deposition, diamond film coalesces together to cover the entire pre-seeded substrate surface [20]. Due to the very slow growth rates (5–50 nm/h) during the LA-MPCVD process, all the articles cited above have reported the growth of continuous nanocrystalline diamond (NCD) films over long (8–20 h) deposition periods. However, there is little or no information about diamond growth behavior during the first hour of LA-MPCVD processing. Nor are there any data over the time period which should be allowed to effectively cover the substrate surface under LA-MPCVD processing conditions [21,22]. The primary obstacle in chemically synthesizing diamond is the fact that the starting point should be diamond itself, as seed particles. Without the appropriate nucleating agent, diamond growth incubation time can be very long, and researchers have tried many methods for nucleation enhancement during CVD growth of diamond [23–27]. Mechanical or ultrasonic scratching of the substrates with abrasives [28,29] and detonation nanodiamond (DND) seeding [30,31] are the most used techniques for promoting nucleation of diamond films before starting the CVD process. However, there are very few reports of nucleation enhancement by electrophoretic deposition (EPD) [32–35]. Here, two seeding techniques have been attempted for the first time: both the EPD- and DND-seeding techniques for nucleation enhancement on different substrates.

Potocky et al. [36,37] also investigated the growth of carbon nanotubes (CNTs) using a linear antenna CVD system with RF biasing of the substrate for 10 min and 40 min durations. Another paper, from the same research group [18], reported LA-MPCVD plasma treatment of polymer passivated NCD layers for enhancement of the diamond surface conductivity by surface hydrogenation. Their research showed that 200 °C is the optimum substrate temperature to effectively hydrogenate the NCD surface without simultaneously damaging the metallic contacts or the top polymeric resist layer used for electronics. Potocky et al. [36] concluded that CNTs grown using LA-MPCVD are hydrophobic, with a contact angle greater than 130°. They used oxygen plasma treatment for 5 min, to enhance the CNT surface wettability. However, they did not attempt to grow diamond films on top of their CNTs [38], which has so far been attempted by the researchers with limited success. It has been reported that CNTs covered with NCDs are better field effect transmitters [39,40]. In the present work, CNTs were grown separately using a thermal CVD reactor on Si substrates, before performing LA-MPCVD of the diamond films onto them. However, being hydrophobic, CNTs could not be seeded (essential for growing diamond using CVD) with water-based DND solution, as could be done for other regular hydrophilic silicon or sapphire substrates. Therefore, EPD was used for seeding the CNT/Si substrate with nanodiamonds for further diamond growth using LA-MPCVD. Such diamond-coated CNTs will have applications in electron field emission.

## 2. Materials and Methods

### 2.1. Substrates

Silicon and sapphire substrates, laser cut into 10 × 10 mm<sup>2</sup> sizes, were used for CVD diamond growth. Silicon substrates were cut out from a p-type 0.5 mm thick 4-inch wafers with a resistivity of 20 ohm cm. Sapphire substrates were single crystal wafers from the commercial supplier Kyocera Global. Both were seeded with nanodiamonds to enhance the diamond nucleation during CVD growth as described in Section 2.1.1.

#### 2.1.1. DND Seeding

Water-based detonation nanodiamond (DND) slurry was spin-coated on top of the silicon and sapphire substrates with a rotating speed of 4000 rpm using a spin coater (Laurell Technologies Corporation, Lansdale, PA, USA, model WS-400B-6NPP/LITE) for

40 s, along with brief rinsing with distilled water, until the surfaces become completely dry [41]. Such monolayer-seeded substrates were then loaded into the LA-MPCVD chamber. Figure 1a is the SEM image of the DND-seeded silicon substrate. The nucleation density was calculated to be  $2 \times 10^{10}/\text{cm}^2$ . Figure 1b is the X-ray diffraction of the as-received sapphire substrate (before DND seeding) used in this study.

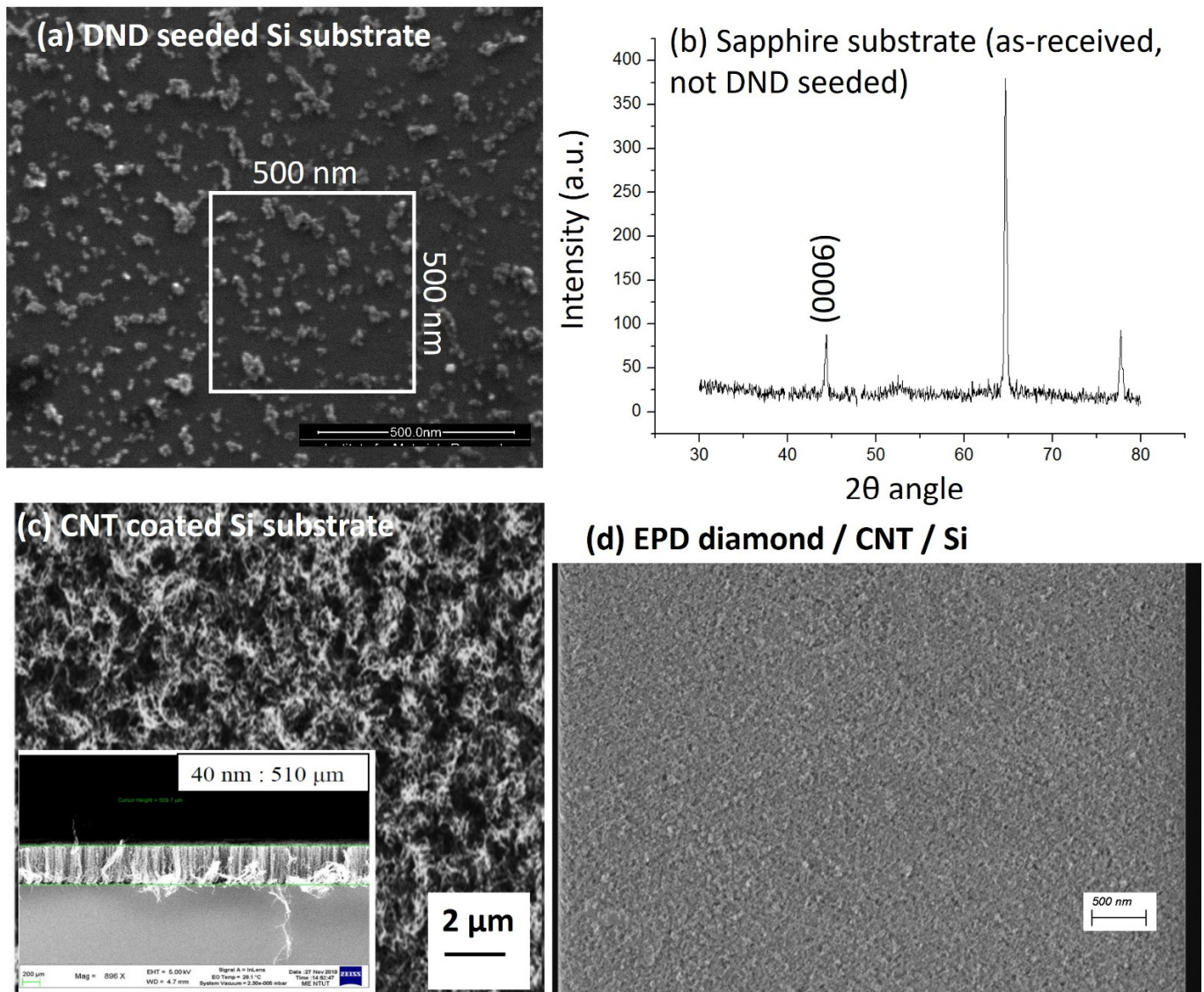


**Figure 1.** Four sets of substrates used in this study: (a) SEM image of the DND-seeded silicon substrate; (b) XRD of sapphire substrate (before DND seeding); (c) CNT-coated silicon substrate, inset SEM showing cross-sectional CNT length; and (d) top view of the EPD of diamond nanoparticles on the CNT/Si substrate.

### 2.1.2. CNT and EPD

Other than the conventional DND seeding procedure, two separate sets of silicon substrates were also prepared. One set of substrates was carbon nanotubes (CNTs) deposited on silicon wafers using iron catalyst-assisted thermal CVD. The other set was prepared by further electrophoretically depositing diamond on top of such CNT/Si substrates.

The growth conditions of CNTs were a working pressure of 3 Torr, a growth time of 20 min at 750 °C with gas flow rates of  $\text{NH}_3$  and  $\text{C}_2\text{H}_2$  of 10 sccm and 40 sccm, respectively. Figure 1c shows the SEM image of the top surface of the CNT/Si substrate. The length of the CNTs was found to be 510  $\mu\text{m}$  (inset).

To protect the CNTs from plasma damage during deposition of the diamond film, the diamond nanoparticles were coated on top of the CNTs using electrophoretic deposition (EPD). In the EPD process, water-based nanodiamond solution (Nanoseed 18 by Micro Diamant AG, Port, Switzerland) was used. The earlier prepared CNT/Si substrates were biased at about +20 V with respect to the reference electrode, the Pt, for 20 s. Figure 1d shows the SEM photograph of the diamond nanoparticles on top of the CNT/Si substrate. The nucleation density was estimated at about  $4.7 \times 10^{10}/\text{cm}^2$ .

## 2.2. LA-MPCVD

All four sets of substrates were loaded together inside the linear antenna microwave plasma-enhanced CVD chamber. No heater was used for additional heating of the substrates. Total volume of the process gases was fixed at 150 sccm and, therefore, the working pressure was also fixed at 0.23 mbar. The base pressure achieved before starting the deposition run was in the order of  $10^{-4}$  Torr. The experimental conditions are described in the following Table 1.

**Table 1.** Process parameters of the samples deposited using LA-MPCVD.

Sample id	Time (min.)	Substrate Temperature (°C)	Heating Rate (°C/min)	NCD Growth Size (nm)	H <sub>2</sub> /CH <sub>4</sub> /CO <sub>2</sub> (%)	MW Power (W)	Pulse Mode (Frequency, Duty Cycle)	Quartz-Tube-to-Substrate Distance (cm)
LA200519-1	60	21–284	4.4	140 (sapphire)				
LA200519-2	30	108–272	5.5	30–70 (silicon)		1500		5
LA200519-3	15	111–236	8.3	-			NO	
LA200520-1	60	21–242	3.7	120 (sapphire)				5
LA200520-2	120	Stable 263	-	20–120 (sapphire)	89/5/6	1100		6.5
LA200525-1	60	21–290	4.5	45–70 (sapphire) 40–90 (silicon)		300 input/ 2000 output	YES, 20 kHz, 45%	5
LA200525-2		126–307	3	10–100 (silicon)				6.5
LA200526-1	15	21–178	10.5	30 (silicon) 20–60 (sapphire)				5
LA200526-2	30	108–272	5.5	45 (silicon) 25–100 (sapphire)	97/3/0	1500	NO	6.5
LA200605-1		21–170	9.9	-	96/4/0			
LA200605-2	15	70–200	8.6	-				5
LA200605-3	11	88–270	16.5	-	95/5/0	2800		

Deposition periods were varied from 11–120 min. The substrates were solely heated by the microwave plasma; therefore, depending on the individual CVD period, the substrate stage temperatures were different, as described in Table 1. For example, sample # LA200519-1 was loaded at a room temperature of 21 °C inside the LA-MPCVD chamber and, after achieving the base pressure of  $7 \times 10^{-4}$  Torr, the plasma was ignited with the introduction

of the processing gases. An average power of 1500 W was achieved by switching on two 2.45 GHz magnetrons. The deposition was carried out for 60 min and the final temperature recorded was 284 °C. It is to be noted that the substrate stage temperature continues to rise during the whole deposition period and the LA-MPCVD plasma heating profiles are depicted in Figure 2. After each CVD run was over, the plasma was put off by disconnecting power supplies to the magnetrons and only the hydrogen gas was allowed to flow through, in order to cool down the substrate stage below 140 °C (permissible temperature safety limit of the reactor), before unloading and loading the next set of 4 substrates. An example of the LA-MPCVD cycle of cooling with hydrogen gas flow, the plasma heating thereafter (11 min long for sample # LA200605-3), and again the successive cooling profile are shown in Figure 2b. However, if the deposition time is long enough, such as for sample # LA200520-2, the temperature profile looks very much stable and flat at 263 °C towards the end of the LA-MPCVD run, as shown in Figure 2c. Table 1 describes widely variable heating rates because of the non-linear nature of the respective heating profiles by the plasma. During the initial LA-MPCVD periods, the temperature rise was steeper, slowing down thereafter to a flatter curve (Figure 2a), before achieving a flat stable temperature regime (Figure 2c). Figure 2d describes the plasma heating of the four samples together during the LA-MPCVD run. The processing was either with CO<sub>2</sub> or without CO<sub>2</sub> gas in the precursor recipe, as shown in Table 1. The reactor chamber was intermittently plasma cleaned by flowing 200 sccm oxygen at 2800 W average input microwave power, for a time duration matching the previously concluded CVD run period. The minimum duration of the CVD run was 11 min, whereas the maximum CVD time was 2 h long in the current set of experiments. The distances were 5 and 6.5 cm between the substrate stage and the linear antenna quartz tube, as determined by trial and error, for optimum NCD film generation. The microwave input power was mostly in continuous wave (CW) mode, except for one set of experiments (sample # LA200525), in which pulsed mode input microwave power was applied at 20 kHz frequency and 45% duty cycle.

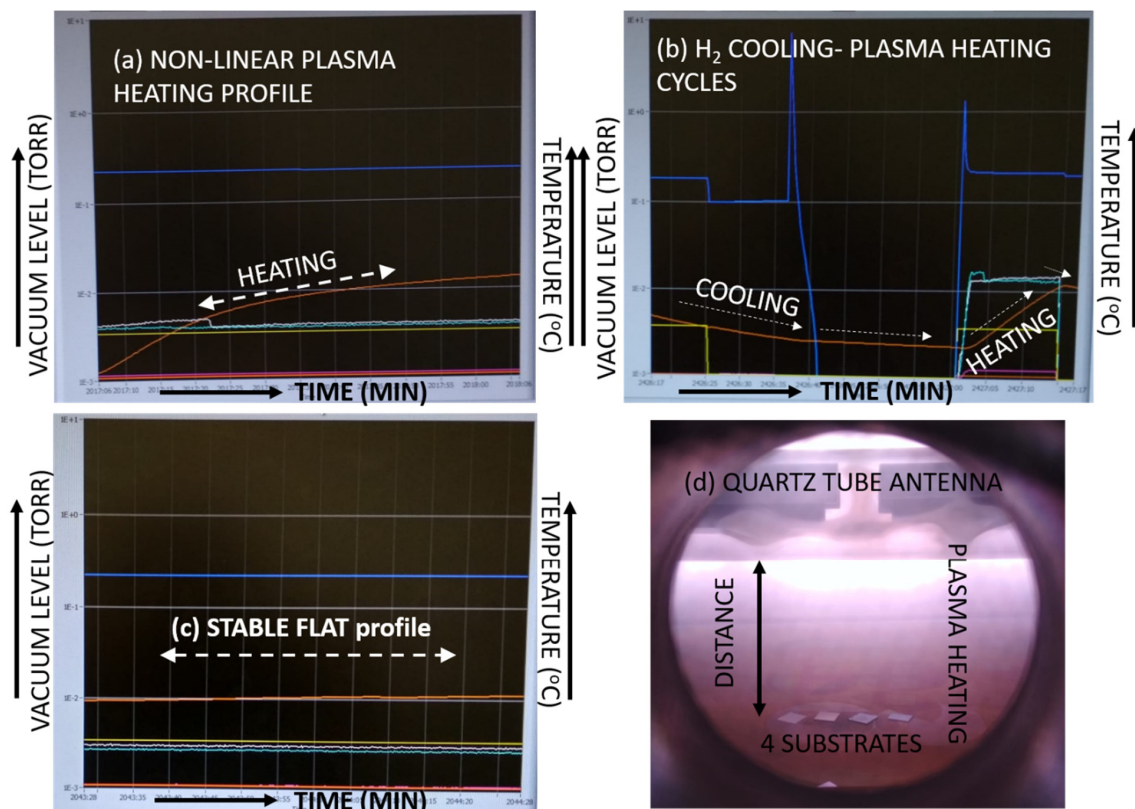


**Figure 2.** Computer screenshots during LA-MPCVD, showing (a) 60 min long plasma heating for sample # LA200519-1, (b) cooling–heating cycle for sample # LA200605-3, with 11 min of short CVD

deposition, (c) stable profiles for 120 min long run with sample # LA200520-2, and (d) view of the microwave plasma heating of the Si, sapphire, CNT/Si, and EPD-diamond/CNT/Si substrates kept together.

### 2.3. Physical Characterisations

The samples were examined using a scanning electron microscope (SEM-FEI Quanta 200 FEG) for evaluating the effects of different processing conditions of the CVD diamond growth. Raman spectroscopy (HORIBA Jobin Yvon T64000 spectrometer using laser light of 488 nm wavelength) was also used to confirm the presence of nanodiamond film. X-ray diffraction (XRD) was used to obtain the characteristic substrate peaks for sapphire.

## 3. Results and Discussion

In this work, silicon and sapphire substrates have been seeded following a standard DND monolayer dispersion technique [41] before growing diamond using LA-MPCVD [15]. Another set of substrates with CNTs on silicon was also prepared for LA-MPCVD diamond growth. A conventional water-based DND suspension could not be used for seeding the CNT/Si substrates since the as-grown CNTs were hydrophobic. Therefore, EPD was used to seed the CNT/Si substrate for nucleation enhancement, reported here for the first time, before LA-MPCVD growth. It is expected that EPD-treated diamond will be a better template for diamond growth than untreated CNT/Si substrate for growing diamond inside the LA-MPCVD reactor.

### 3.1. First Hour of LA-MPCVD Growth

#### 3.1.1. Silicon Substrates

Figure 3 compares the NCD growth patterns after 15, 30, and 60 min of LA-MPCVD runs. Figure 3a,b,d show a gradual increase in the size of the diamond nanocrystals with increasing deposition time. After the first 15 min of LA-MPCVD, the nanodiamond seed crystals, which are typically 4–6 nm in size, or their agglomerates (Figure 1a) grew into bigger sizes but did not become large enough to effectively touch each other in order to form a connecting network of diamond nanocrystals (Figure 3a—the current SEM image magnification was not high enough to determine the respective NCD sizes after 15 min of LA-MPCVD growth). As the deposition time is increased to 30 min and further to 60 min of LA-MPCVD, the diamond nanocrystals start touching each other but still not enough to completely cover the underlying silicon substrate. The black contrasting substrate features are gradually found to diminish in the corresponding SEM images (Figure 3a,b,d, respectively). It was easier to calculate the uncovered substrate surface areas than the size of the individual NCDs grown over them after 15 min of LA-MPCVD. The average lengths of the uncovered silicon substrate areas were more than 270 nm (Figure 3a) after 15 min of the LA-MPCVD run, and were reduced (but not enough to let the nanodiamond crystals touch each other) after 30 min of LA-MPCVD, as shown in Figure 3e. The sizes of the nanodiamond seed crystals are found to grow to about 30 nm for isolated nanocrystals or to sizes of 60–70 nm for their agglomerates, shown in Figure 3e. Even after 60 min of LA-MPCVD, 150–200 nm long uncovered silicon areas were still visible in Figure 3d. It is important to note that the 30 nm or 70 nm NCDs, shown in Figure 3e, are actually agglomerations of tinier (about 10 nm) nanoparticles.

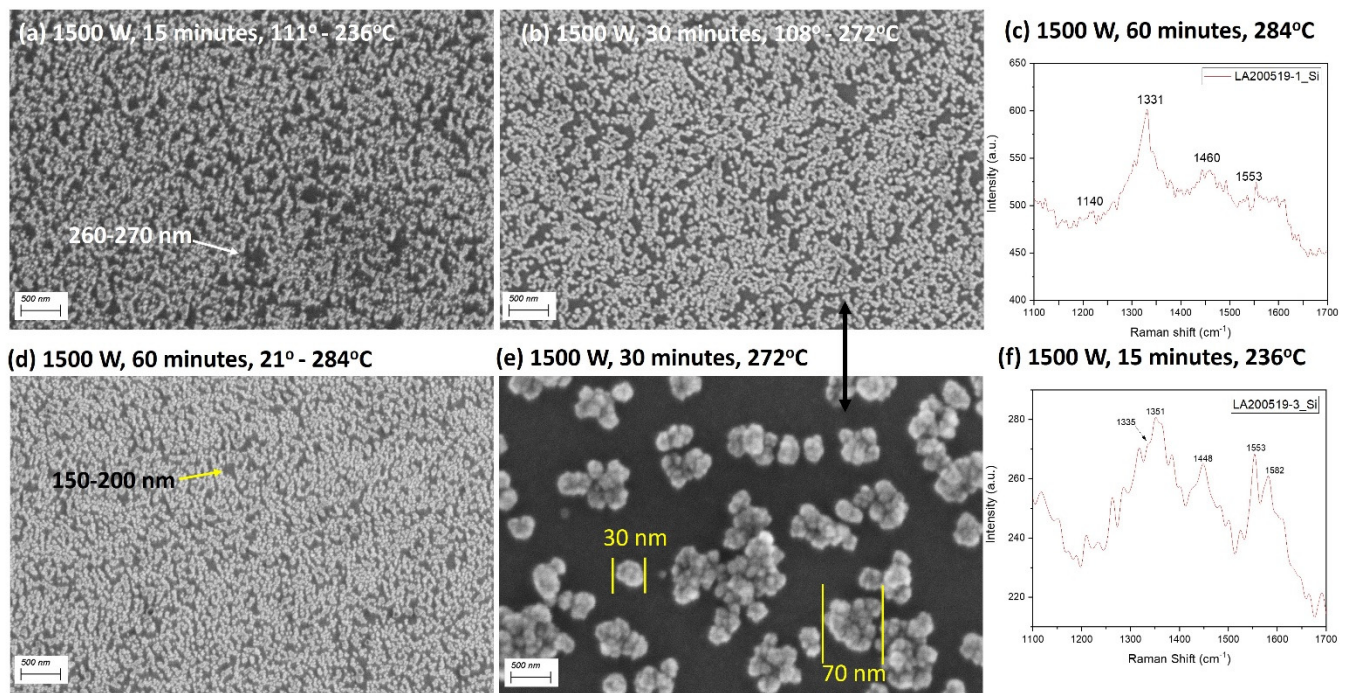


**Figure 3.** NCD crystals on DND-seeded silicon substrates. (a) SEM of the sample grown after first 15 min, (b) SEM of the sample grown after 30 min at  $20\times$  magnification, (c) Raman spectra of the sample grown after 60 min, (d) SEM of the sample grown after 60 min, (e) SEM of the sample grown after 30 min at  $200\times$  magnification, and (f) Raman spectra of the sample grown after 15 min of LA-MPCVD growth.

The Raman spectra from the diamond nanocrystals after 15 min of LA-MPCVD is found to be very noisy (Figure 3f), with a small  $sp^3$  peak at  $1335\text{ cm}^{-1}$  in contrast to the disordered graphite (D) band at  $1351\text{ cm}^{-1}$ . There are also Raman peaks at  $1448$ ,  $1553$ , and  $1582\text{ cm}^{-1}$ , which correspond to trans-poly-acetylene (TPA) and graphite crystals (G), respectively, in the growing NCD film. On the other hand, the  $sp^3$  Raman signal after 60 min of LA-MPCVD diamond growth is found to be very strong ( $I_{sp^3} = 156$ ) with a FWHM of  $18\text{ cm}^{-1}$  (Figure 3c). The corresponding non-diamond Raman peaks for TPA ( $1140$  and  $1480\text{ cm}^{-1}$ ) and G-band ( $1553\text{ cm}^{-1}$  and hump thereafter) are also present but at a much-reduced level ( $I_{sp^2} = 60$ ), indicating the growth of good quality diamond nanocrystals. The  $sp^3$  Raman peak signal enhancement in Figure 3c in comparison to Figure 3f is due to the combined effect of increased LA-MPCVD deposition time, which also helped to achieve higher substrate temperatures. It is important to note that the NCD growth temperature is dynamic and continuously increasing during the deposition time over which the stage was allowed to be heated by the microwave plasma. The longer the CVD run time, the higher the substrate temperature, until the substrate temperature becomes gradually stable with the progressing time. A total of 15–60 min of heating by the plasma does not allow the substrate temperature to become stabilized (Figure 2a).

### 3.1.2. Sapphire Substrates

Figure 4 shows the corresponding Raman spectra from the NCDs grown over DND-seeded sapphire substrates, kept alongside the silicon substrates as shown in Figure 2d. Here it is also found that the  $sp^3$  Raman peak in and around  $1331\text{ cm}^{-1}$  is the sharpest, with a FWHM of  $15\text{ cm}^{-1}$  (Figure 4a), from the NCDs grown over the longer run time of 60 min. In fact, NCDs grown over sapphire substrate have better FWHM values than NCDs grown over silicon substrates (Figure 3c). The  $sp^3$  Raman signals become gradually weaker (Figure 4b,c) and other non-diamond peaks (TPA— $1491$ , graphitic D— $1350$ , and

G—1600  $\text{cm}^{-1}$ ) become stronger due to the presence of smaller NCDs, with the reduction in LACVD time periods.

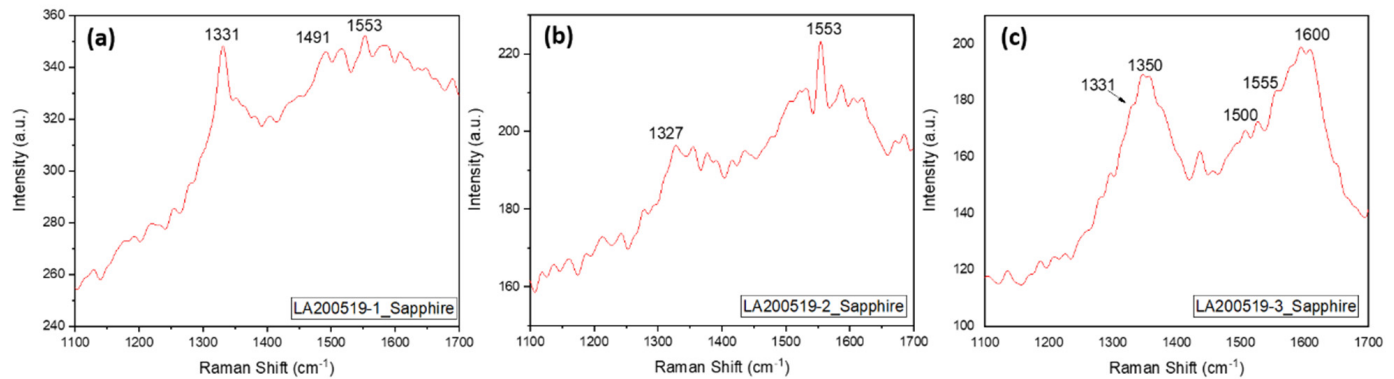


**Figure 4.** Raman signals from the NCD crystals grown over DND-seeded sapphire substrates after (a) 60, (b) 30, and (c) 15 min of LA-MPCVD growth at 1500 W power, 5 cm stage-to-antenna distance with gas recipe of  $\text{H}_2/\text{CH}_4/\text{CO}_2 = 89/5/6$ .

### 3.1.3. CNT and EPD Substrates

The SEM and Raman spectroscopy results from the CNT/Si and EPD-diamond/CNT/Si substrates kept alongside the silicon and sapphire DND-seeded substrates after 15 min of LA-MPCVD processing are shown in Figure 5. Longer CVD growth periods of 30 and 60 min were completely etching the CNTs due to the oxidation by the microwave plasma recipe of  $\text{H}_2/\text{CH}_4/\text{CO}_2 = 89/5/6$ . The well-connected CNT network shown in Figure 1c is found to be etched completely by the LA-MPCVD plasma even after 15 min into the deposition period, as shown in Figure 5a,d. However, the EPD-treated CNT/Si substrate is found to be less affected by the LA-MPCVD plasma, as the length of individual CNTs are found to be longer ( $>20 \mu\text{m}$ ) in Figure 5a than in Figure 5d ( $<5 \mu\text{m}$ ). Figure 5b is the higher magnification image of Figure 5a, taken from the intermediate region of the individual CNTs. It shows that the substrate surface is fully covered with carbonaceous film. The Raman signal of such film is shown in Figure 5c with a stronger  $\text{sp}^3$  signal at  $1335 \text{ cm}^{-1}$  along with another less intense peak at  $1559 \text{ cm}^{-1}$  for graphitic carbon. Figure 5b consists of tiny individual NCD grains (20–60 nm) present all over the EPD-diamond/CNT/Si plasma-treated surface, along with square-shaped holes (140–280 nm). Such rectangular or square holes are also present on the CNT/Si plasma-treated surface (Figure 5e) but are much smaller in size (50–100 nm). Correspondingly, the individual diamond nanoparticles that are present all over the substrate surface in Figure 5e are also smaller in size (20–40 nm) than those found in Figure 5b. Similarly, the  $\text{sp}^3$  ( $1334 \text{ cm}^{-1}$ ) and graphitic ( $1588 \text{ cm}^{-1}$ ) carbon signals from the plasma-treated CNT/Si surface (Figure 5f) are also weaker, and peaks are present at  $1453 \text{ cm}^{-1}$ , which are due to trans-polyacetylene (TPA). TPA is formed at grain boundaries and at the surface of NCD films, as evidenced by the characteristic Raman bands of  $\nu_3$  (C–H in plane bending) around  $1150 \text{ cm}^{-1}$  and  $\nu_1$  (C=C stretch) around  $1480 \text{ cm}^{-1}$  [42]. Hu et al. proposed a possible role of TPA in diamond synthesis which is yet to be explored in detail. The presence of the  $\text{sp}^3$  Raman signal from the LA-MPCVD plasma-treated CNT/Si substrates confirms the fact that, even without nanodiamond seeding, it is possible to deposit NCDs on top of CNTs. This is because the gas phase nucleation rate of diamond under the low electron temperature of LA-MPCVD plasma is higher than the etching rate of the precipitated diamond at low substrate temperature [43].



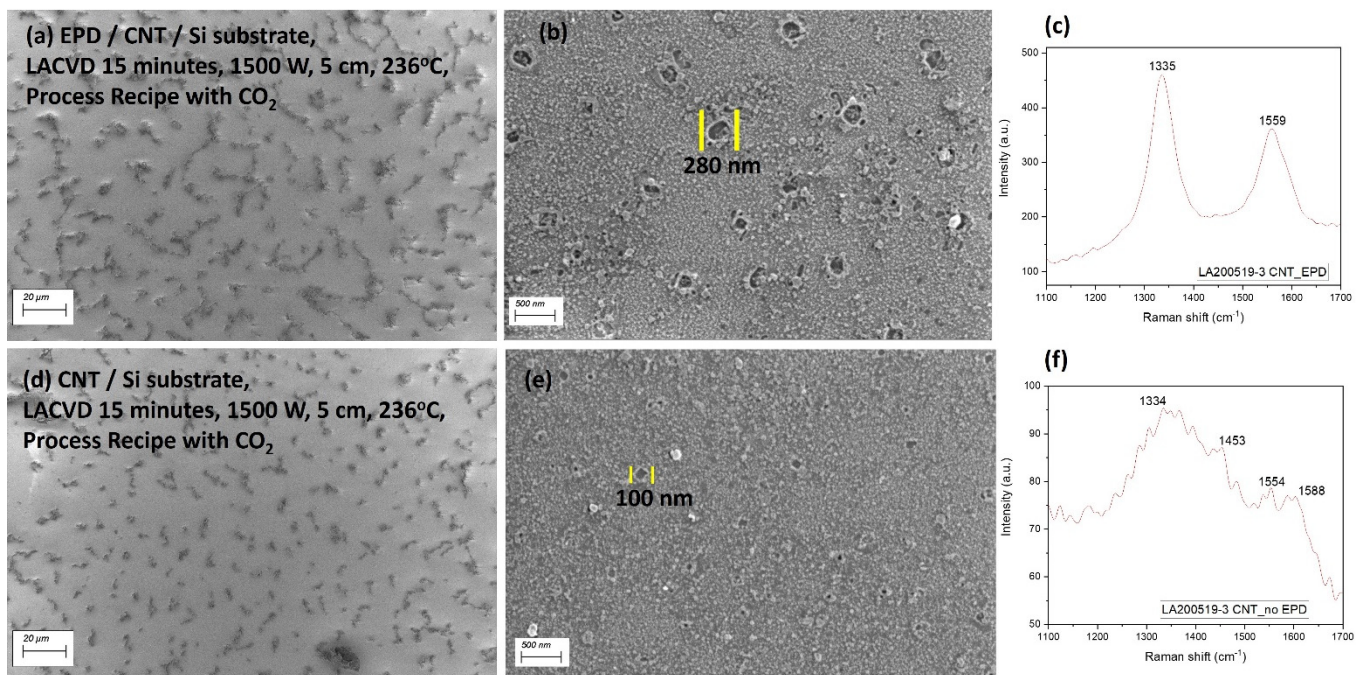


**Figure 5.** Please refer to Table 1, row 4, process conditions, after 15 min of LA-MPCVD plasma treatment: (a) SEM at 500× magnification; (b) 20 k× magnification; and (c) Raman signal of EPD-diamond CNT/Si substrate after 15 min of LA-MPCVD plasma treatment. (d) SEM at 500× magnification, and (e) 20 k× magnification, and (f) Raman signal of CNT/Si substrate.

There are a few white particles that are found to be present inside the rectangular holes (Figure 5b,e). The holes might have been created by the dislodgment of such white particles. Thus, it is found that the EPD-treated CNTs are burnt to a lesser extent by the LA-MPCVD plasma (comparing Figure 5a,b). Moreover, it is also possible to grow CVD diamond onto CNT/Si substrate without the need for nanodiamond seeding (Figure 5f).

### 3.2. Low MW Power

The substrate temperatures that can be achieved inside the LA-MPCVD reactor, solely by means of plasma heating, depend on the input MW power and also on the stage-to-antenna distances. Therefore, in the next set of experiments, the MW power was reduced to 1100 W and the stage-to-antenna distances were varied from 5 to 6.5 cm, in order to see their effect on the growth of nanodiamond crystals during the early periods of LA-MPCVD. The lowest possible substrate temperature (15 h of deposition) that Izak et al. [14] could achieve was 250 °C, by lowering the input microwave power to 1200 W. They also used higher input MW powers of 1700 W and 2500 W. However, they did not mention the substrate-to-antenna distance used in their experiments. Reportedly [11,16,22], it is kept at an optimal distance of 5–7 cm to achieve a stable substrate temperature of 400–450 °C by plasma heating. Closer distances, such as 4 cm, could produce substrate temperatures of 550 °C. In order to achieve higher substrate temperatures (>600 °C), a resistive heater is usually used underneath the substrate.

The substrate temperature continues to rise from room temperature to 242 °C, at the end of a one-hour long LA-MPCVD run (Table 1, sample # LA200520–1). Surprisingly, at the lower MW of 1100 W, the NCDs were found to almost cover the entire silicon substrate (Figure 6a), which was not observed even at 1500 W (Figure 3d). A higher magnification SEM image in Figure 6b reveals the NCD sizes to be around 40–100 nm. Still, there are intermediate bare substrate areas visible in between the NCD grains. There is no evidence of secondary nucleation. The NCDs seem to grow in the lateral direction to cover the substrate surface with a single-layer coalescing film.

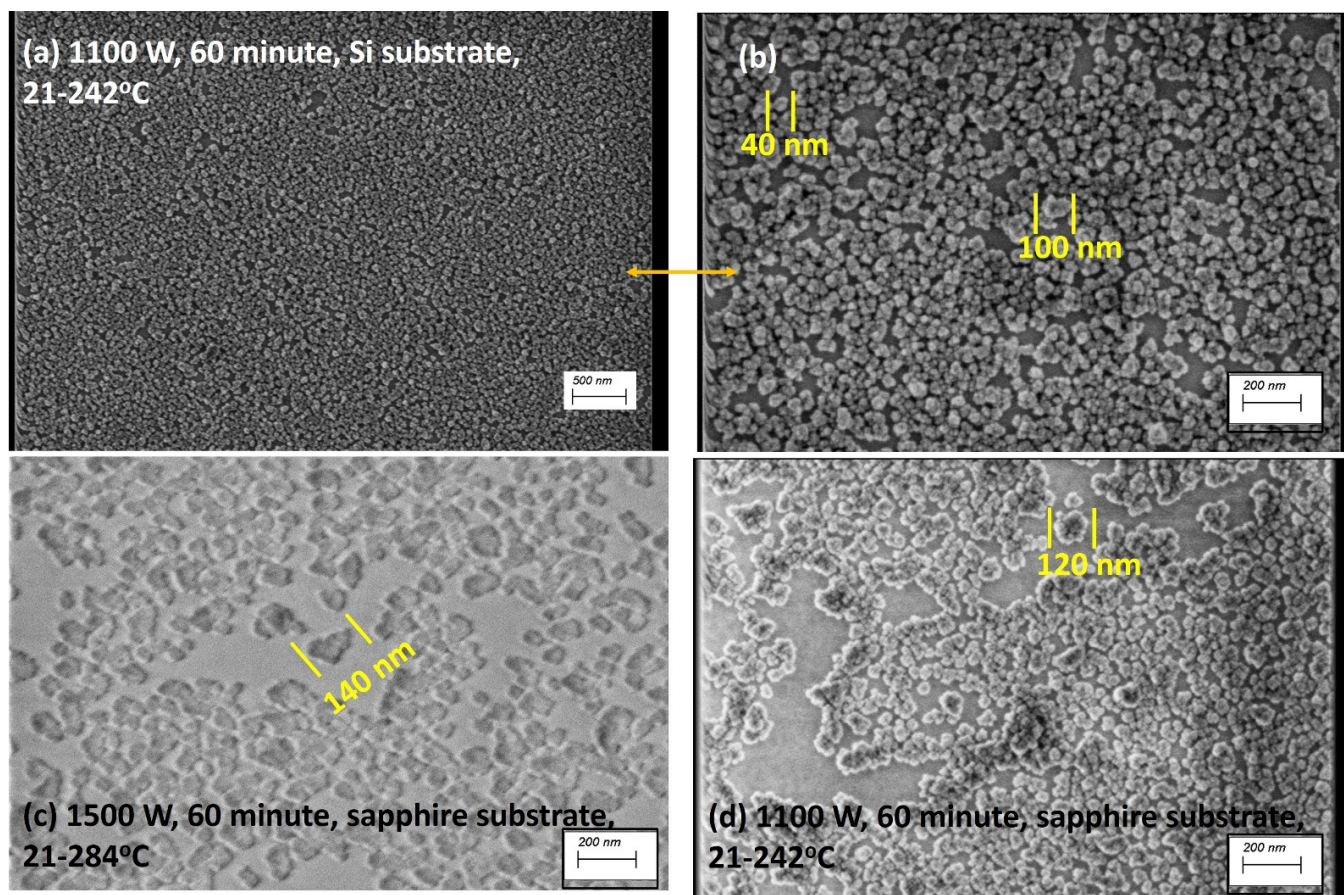


**Figure 6.** Nearly coalesced NCD crystals grown using a LA-MPCVD reactor at a reduced power level of 1100 W on silicon substrate for 60 min: (a) 20 k $\times$  and (b) 50 k $\times$  magnification SEM images. Comparison of diamond nanocrystal coalescence on sapphire substrates after 60 min of LA-MPCVD at MW power levels of (c) 1500 W, isolated, and (d) 1100 W, connected.

Figure 6c (sapphire sample # LA200519–1) and 6d (sapphire sample # LA200520-1) compare the effect of lowering the input MW power on the diamond growth behavior during the first 60 min of LA-MPCVD processing with identical stage-to-antenna distances of 5 cm. An input MW power of 1500 W seems only to heat the substrate to a higher temperature of 284  $^{\circ}$ C, starting from room temperature, but the higher power did not help in effective grain coalescence, as seems to be possible with 1100 W power, as shown in Figure 6d. The sizes of the NCDs are comparable between Figure 6c (approximately 140 nm NCDs scattered and isolated from each other) and 6d (about 120 nm NCD agglomerates). However, at lower power, the grains are more coalesced and interconnected (Figure 6d). It appears that lower input power is beneficial to lateral growth of the diamond nanocrystals. There is still no sign of secondary nucleation.

### 3.3. Pulse Mode MW Power

Pulse mode operation of the LA-MPCVD reactor helps in achieving better quality diamond crystals with further reduction in input power level [13]. When the input MW power was 300 W, at 20 kHz pulse frequency and 45% duty cycles, the average output MW power recorded was 2000 W (Table 1). During the first hour of the LA-MPCVD run for sample # LA200525-1, the substrate temperature continued to rise from room temperature to 290  $^{\circ}$ C (similar to 1500 W, sample # LA200519-1) at a stage-to-antenna distance of 5 cm; however, after stopping the first run at the end of 60 min, the substrate was allowed to cool down to 140  $^{\circ}$ C (reactor component safety temperature limit before opening the chamber door) before loading the second set of samples (sample # LA200525-2). Therefore, the

starting temperature for the second run (sample # LA200525-2) was 126 °C—it was not the room temperature, as it was for the previous first run (sample # LA200525-1). A LA-MPCVD starting temperature of 126 °C enables the substrate temperature to attain an even higher value of 307 °C after 60 min of plasma heating, even at a longer stage-to-antenna distance of 6.5 cm.

Figure 7 shows the lower (5 k $\times$ —Figure 7a,c) and higher magnification (50 k $\times$ —Figure 7b,d) images of the silicon and sapphire substrates from the LA-MPCVD run with sample # LA200525-1. It is found that pulse mode helped in producing denser film coverage of the silicon substrate (Figure 7a,b) surfaces in comparison to the 1500 W (# LA200519-1, Figure 3d) continuous mode input MW power runs after 1 h of LA-MPCVD. However, if Figure 7a,c are compared, it appears that the sapphire substrates are more successfully covered (less contrasting black substrate areas) with diamond nanocrystals. However, their respective higher magnification images reveal that the sizes of the nanodiamonds are somewhat bigger (40–90 nm) on silicon substrates than on the sapphire substrates (45–70 nm), and the respective grain size distribution is also narrower. The NCD sizes may be bigger for silicon substrates, but their densities ( $\approx 7$  NCDs on silicon against  $\approx 12$  NCDs on sapphire over 200 nm  $\times$  200 nm substrate areas) are higher for the sapphire substrates, indicating favorable growth on the sapphire substrates. Still, the pulse mode could not produce continuous NCD films on both the substrates. The primary reason is the unstable (continuously rising, 21–290 °C) substrate temperature, which did not allow growth of nanodiamond crystals, fully covering the substrate surface.

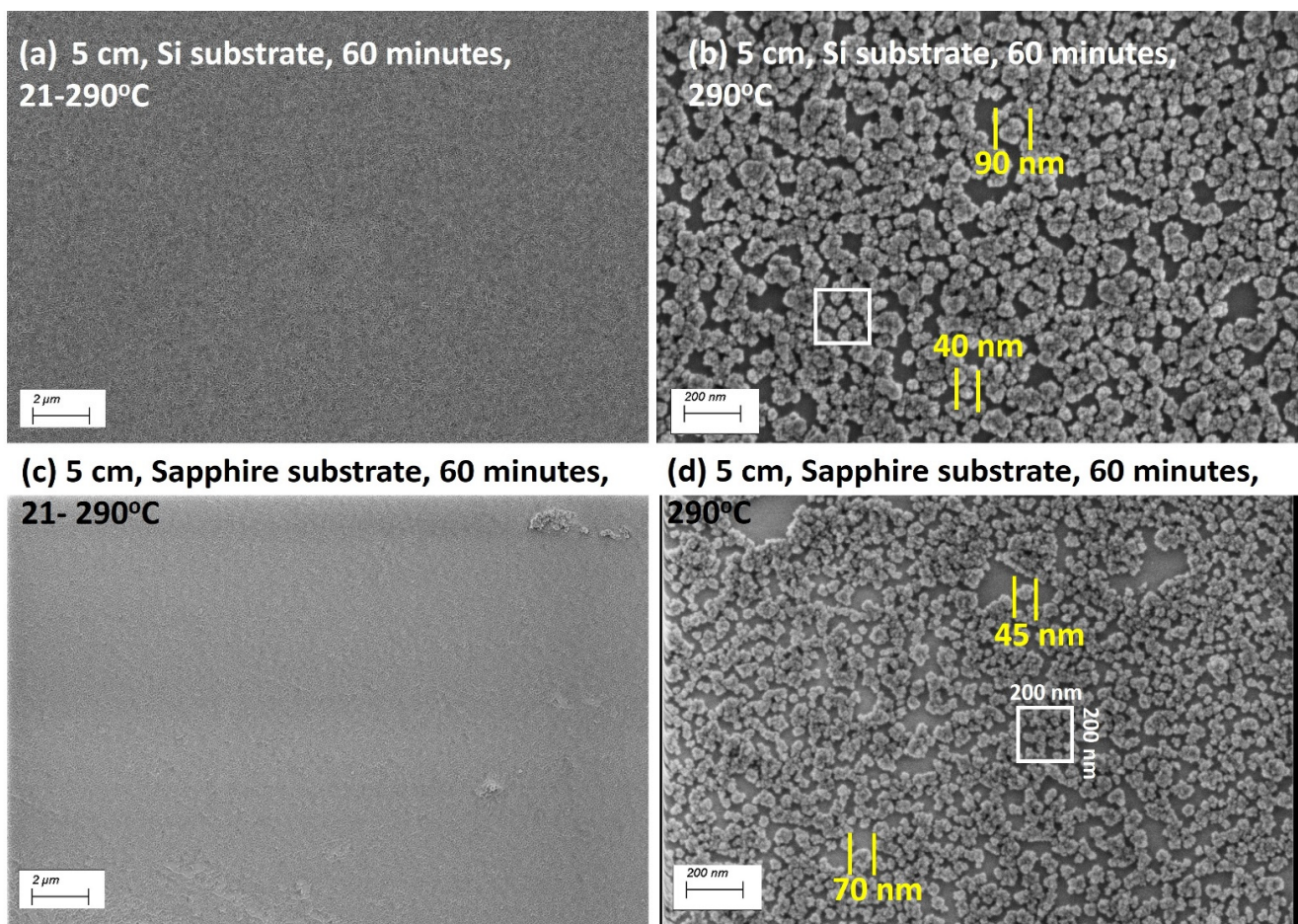


**Figure 7.** SEM images of the NCD films (sample # LA200525-1) grown using pulse mode MW (input 300 W/output 2000 W) power on Si substrates at (a) 5 k $\times$  and (b) 50 k $\times$  magnifications, and on sapphire substrates at (c) 5 k $\times$  and (d) 50 k $\times$  magnifications.

### 3.4. Fully Coalesced NCD Films

It was found that, even after 60 min of LA-MPCVD processing at a higher power of 1500 W or a lower power of 1100 W, or even with pulse mode MW power, at a stage-to-antenna distance of 5 cm, none of the processing conditions could produce continuous diamond films on both the DND-seeded silicon and sapphire substrates. Had this been a conventional resonant cavity microwave plasma CVD reactor, it would have produced continuous micron-thick high-quality NCD films with a  $\text{H}_2/\text{CH}_4/\text{CO}_2 = 89/5/6$  process recipe after 1 h of growth [1]. Next, lowering of the substrate stage to a distance of 6.5 cm away from the linear antenna quartz tube was attempted to lower the substrate temperature. In effect, this was to promote less etching of the deposited films nearer to the antenna, and to produce a continuous film on the substrate surface, even if the diamond will be poorer in quality.

Lowering the stage from 5 cm to 6.5 cm was beneficial to the substrate surface. Figure 8a and its inset, which were the diamond film SEM images on silicon substrate after 1 h LA-MPCVD in pulse mode at 5 cm distance, still show dark contrasting uncovered silicon substrate areas underneath, but the nanodiamond grains are more or less connected with each other without any sign of isolated NCDs. It appears from Figure 8a that the pulse mode was a more effective processing condition in covering the substrate surface with a single layer of NCD film. However, if the distance is increased to 6.5 cm (Figure 8b and inset), there is a sign of secondary nucleation, which may produce poor quality diamond. This indicates that a wider stage-to-antenna distance helped secondary nucleation to take place and produced almost fully covered silicon substrate. The Raman signal from such semi-continuous NCD film on sapphire substrate shows a very high FWHM of  $40\text{ cm}^{-1}$  for the  $\text{sp}^3$  peak at  $1333\text{ cm}^{-1}$ , along with the appearance of the TPA peak at  $1502\text{ cm}^{-1}$  and graphite G peaks at  $1606$  and  $1552\text{ cm}^{-1}$ . The high value of FWHM confirms the presence of secondary nuclei, as is also evident from the SEM image. The end temperature of the second 60 min LA-MPCVD run was somewhat higher at  $307\text{ }^\circ\text{C}$ , as its starting temperature was also higher at  $126\text{ }^\circ\text{C}$ —after the end of the first experiment of 60 min LA-MPCVD, which started from a room temperature of  $21\text{ }^\circ\text{C}$ . However, both were not performed long enough to make the substrate temperature reach a stable flat curve. The substrate temperature was continuously changing (increasing) during both the runs—initially at a faster pace (steep slope) and later at slower (flatter slope) heating rate.

It was found that for sample # LA200520-2, grown at a longer substrate-to-antenna distance of 6.5 cm, and grown for a longer duration of 2 h, the LA-MPCVD process conditions could produce a flat substrate temperature curve, as shown in Figure 2c. The longer distance of 6.5 cm promoted production of secondary nucleation of diamond crystals (wide range of NCD grain sizes from 20–120 nm—Figure 8f) and the longer time of LA-MPCVD allowed the films to coalesce to form full substrate coverage, as shown in Figure 8d–f. Earlier, it was also found that a lower power of 1100 W contributed to producing better film coverage (Figure 6a) than 1500 W on silicon substrate (Figure 3a). Figure 6d is the NCD film after 1 h LA-MPCVD on sapphire, showing the underlying bare substrate, but if the LA-MPCVD was allowed to proceed for another 1 h, it was found to fully cover the sapphire substrate surface (Figure 8e,f). Figure 6d shows a cluster of 12 diamond nanoparticles, with 120 nm total diameter. Although every grain is not of equal dimension, it may be estimated that the individual nanodiamond crystals are 5–10 nm in size. This was the case after 1 h of LA-MPCVD on sapphire substrate, but when the LA-MPCVD proceeded for another 60 min, it was found to produce secondary nucleation with variable nanodiamond sizes of 120, 60, or 30 nm individual grain sizes (Figure 8f). Therefore, longer periods of LA-MPCVD helped to grow the film both laterally and in three dimensions due to secondary nucleation. Researchers have previously reported [22] that there is a high-pressure growth regime, which promotes diamond re-nucleation, and a low-pressure growth regime, which promotes lateral growth. A low electron temperature inside LA-MPCVD is essential for continuous re-nucleation of diamond in hydrogen-rich plasma [43].

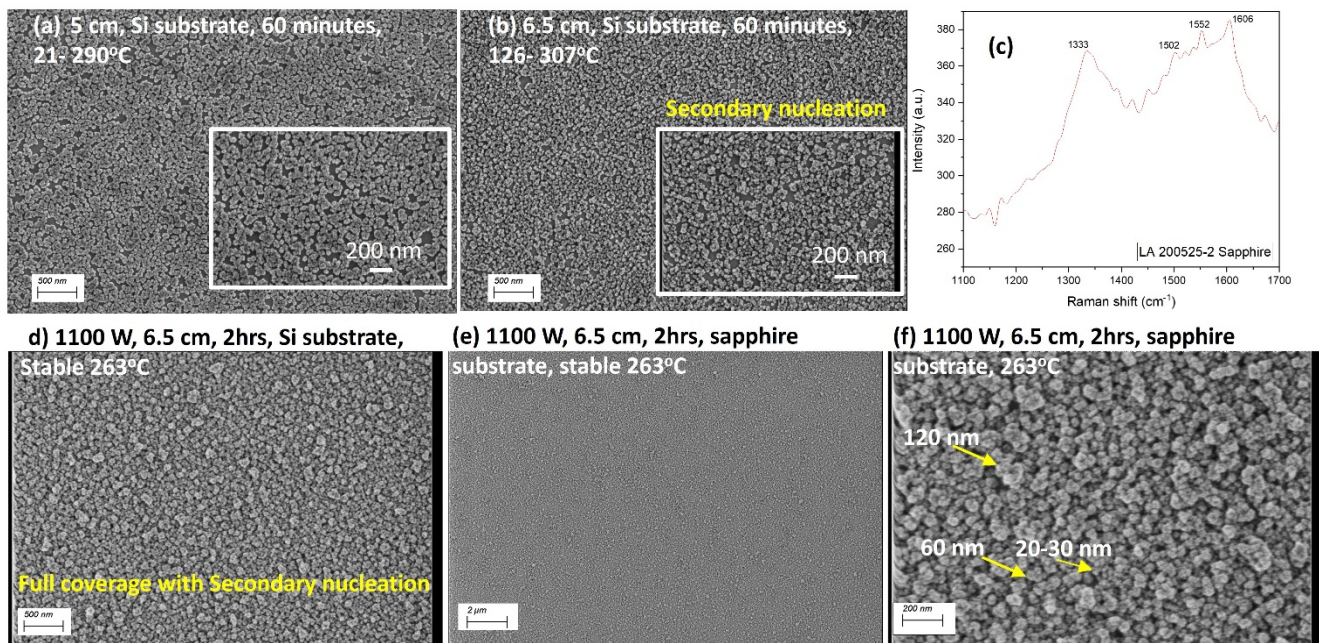


**Figure 8.** Coalescence and secondary nucleation of NCDs. SEM of (a) interconnected NCDs on Si, pulse mode at 5 cm, (b) secondary nucleated NCDs on Si in pulse mode at 6.5 cm, (c) Raman spectra from secondary nucleated NCDs after 1 h LA-MPCVD in pulse mode at 6.5 cm. SEM images of NCDs after 2 h LA-MPCVD in CW mode at 6.5 cm, 1100 W power (d) on Si, and (e) on sapphire substrates, and (f) 50 k $\times$  magnification of image in 8e.

### 3.5. LA-MPCVD Growth without CO<sub>2</sub>

#### 3.5.1. EPD-Diamond/CNT/Si Substrates

It was found that the EPD-treated CNT/Si substrates were also etching out quickly under the LA-MPCVD plasma recipe of H<sub>2</sub>/CH<sub>4</sub>/CO<sub>2</sub> = 89/5/6. Therefore, in order to reduce the effect of oxidation, in the next set of experiments, CO<sub>2</sub> gas was removed from the process recipe. Figure 9a,b show the Raman spectra of the EPD-seeded CNT/Si substrates after 15 and 30 min of LA-MPCVD plasma treatment without CO<sub>2</sub> in the recipe of H<sub>2</sub>/CH<sub>4</sub> = 97/3. It was found that even after 30 min of LA-MPCVD, CNTs survived the plasma conditions (inset Figure 9d). The corresponding Raman signal of the sp<sup>3</sup> peak was weaker than those of the graphitic D-band (Figure 9a) after 15 min of LA-MPCVD; however, the Raman spectra started producing fluorescent signals after 30 min of LA-MPCVD, as shown in Figure 9b. There lies a definitive signal (not prominent enough due to background fluorescence) for diamond at 1330 cm<sup>-1</sup>, which was taken from the sample in Figure 9d. There are loosely scattered diamond nanoparticles, of around 80 nm diameter or less, all throughout the images in Figure 9c,d. There are some occasional appearances of square or rectangular holes in the plasma-treated EPD-diamond/CNT/Si substrate surface. The sizes of those holes vary from 250–350 nm. It is interesting to see that some of the holes were occupied by bright whitish nanoparticles—their dimensions were measured to be 250 nm. It can be assumed that the dislodgment of such white particles resulted in the creation of those square or rectangular holes. The SEM images of Figure 9c,d were taken from the intermediate regions of the individual CNTs (inset image of Figure 9d). The sizes of some of the CNTs were found to be as big as 25  $\mu$ m. If the CNT lengths in Figure 9d are compared with those in Figure 5a (20  $\mu$ m after 15 min LA-MPCVD), it is concluded that even after 30 min of LA-MPCVD plasma treatment, EPD-seeded CNT/Si survived diamond deposition conditions without complete etching, due to the absence of CO<sub>2</sub> in the recipe.

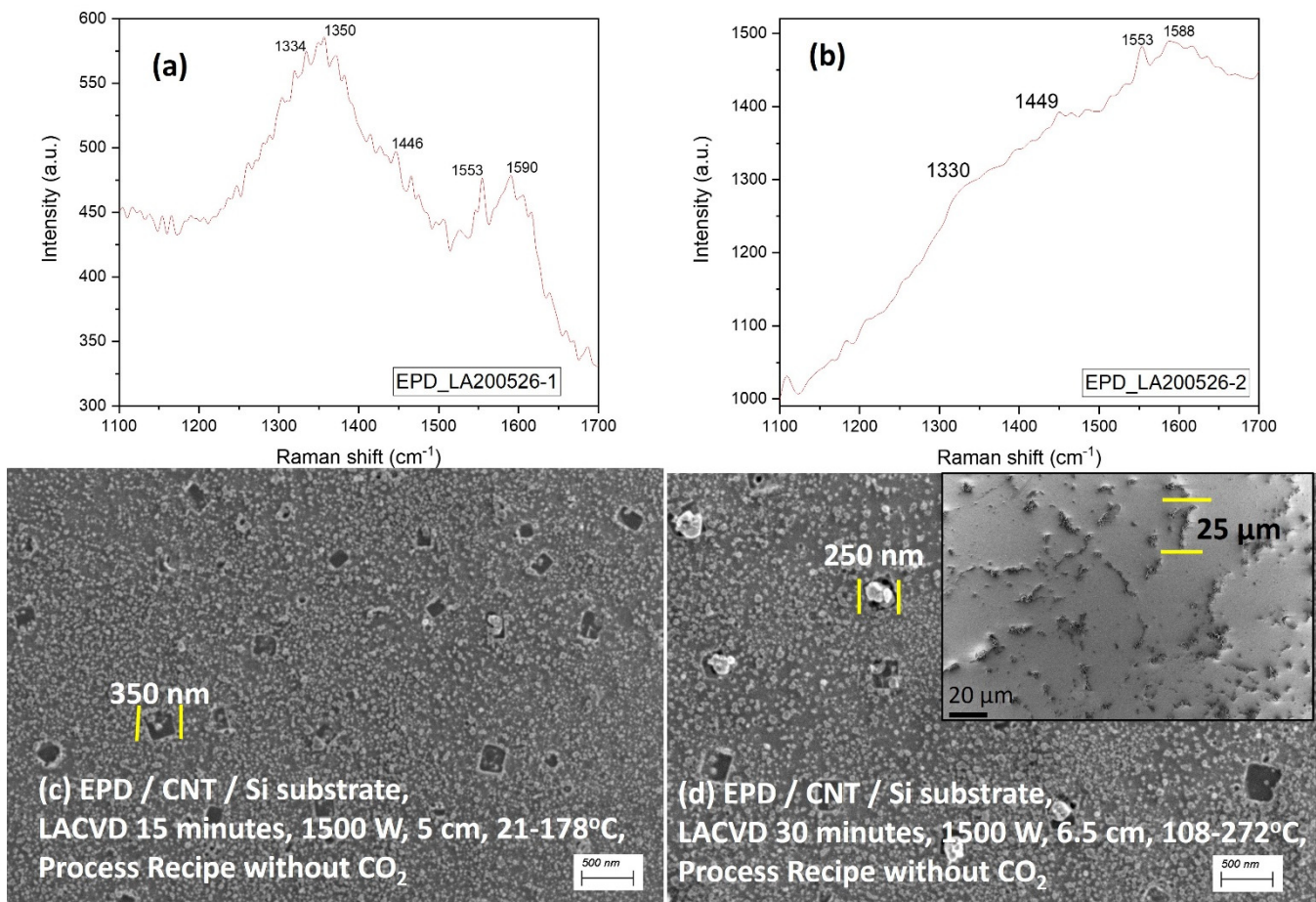


**Figure 9.** Effect of LA-MPCVD plasma processing on EPD-seeded substrates, without CO<sub>2</sub> in the recipe. (a) Raman signal of the sample grown after 15 min, (b) Raman signal of the sample grown after 30 min, (c) top surface SEM at 20 k× magnification of the sample grown after 15 min, and (d) top surface SEM at 20 k× magnification of the sample grown after 30 min, with 500× inset image showing survival of CNTs after plasma treatment.

### 3.5.2. Silicon and Sapphire Substrates Effect of CH<sub>4</sub>

Sections 3.1.1 and 3.1.2 have already shown that the early periods of the low-temperature LA-MPCVD run could not produce fully covered, otherwise perfectly DND-seeded silicon and sapphire substrates (even after 60 min of deposition). One of the reasons for the slow growth of diamond crystals could have been the rapid etching of the nanodiamond films by the CO<sub>2</sub> present in the plasma recipe. Therefore, this was further investigated to observe the effect of removing CO<sub>2</sub> from the recipe during LA-MPCVD nanodiamond growth. Researchers [44] have shown that at a low CO<sub>2</sub> concentration (less than 0.5%), there is formation of SiC in competition with the growth of boron-doped NCDs during the LA-MPCVD process, which is due to silicon contamination from the quartz tube. Moreover, CO<sub>2</sub> (less than 1%) enhances the NCD growth rate (16 nm/h) in continuous mode LA-MPCVD. However, a percentage increase in CO<sub>2</sub> gas over CH<sub>4</sub> gas reduced [11,13] the growth rate (7 nm/h). However, there is no report so far about the effect of CH<sub>4</sub> percentages on the NCD growth pattern, specifically during the unstable periods of the LA-MPCVD run, i.e., until the stable substrate temperature is achieved.

Figure 10a–c are the SEM images of the NCD crystals grown over the Si substrates with increasing methane percentages (3%–5%), after only the first 15 min of LA-MPCVD. It is found that the individual DND seed-crystal sizes (Figure 1a) grew in Figure 10. The diamond nanoparticle density is calculated to be equal to  $0.85 \times 10^{10}/\text{cm}^2$  in Figure 11c

for a 5% CH<sub>4</sub> percentage over silicon substrates, which is to some extent less than that calculated from Figure 1a for the DND seeds ( $2 \times 10^{10}/\text{cm}^2$ ). This demonstrates that, during the early growth stage, the DND seeds only grow laterally in size, and some seed crystals disappear due to plasma etching. The Raman signal from the NCD film on the Si substrate grown at 3% CH<sub>4</sub> after 30 min of LA-MPCVD (Figure 10d) is shown to produce quite a sharp sp<sup>3</sup> peak with a FWHM of 22 cm<sup>-1</sup>. There are also Raman peaks in Figure 10d corresponding to non-diamond carbon depositions at 1541 and 1600 cm<sup>-1</sup>, respectively. It is observed that the dark contrasting Si substrate areas in Figure 10a–c are progressively diminished, indicating that with the increase in the CH<sub>4</sub> percentage, the DND seed crystals grow bigger in size within a given LA-MPCVD run time.

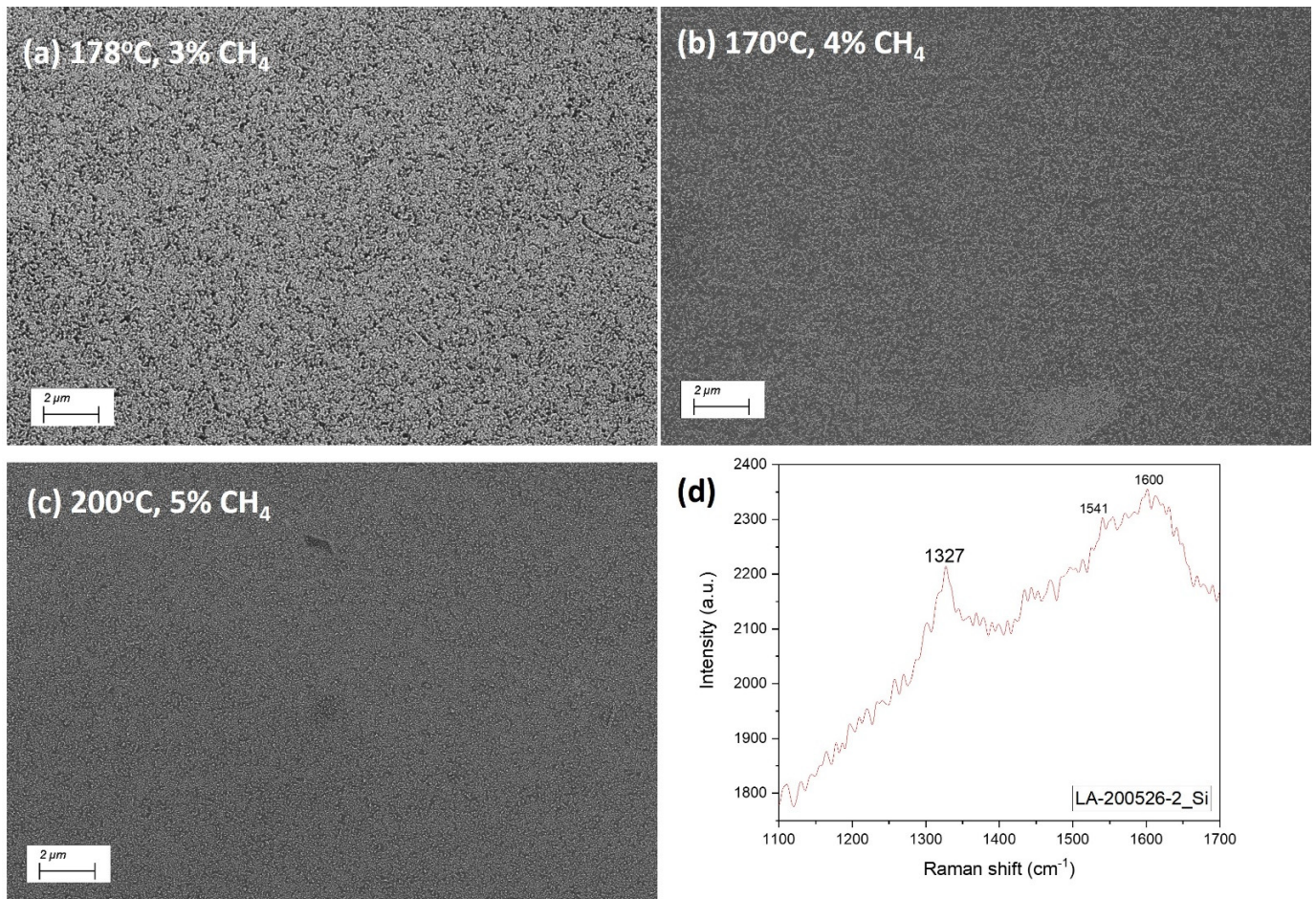


**Figure 10.** LA-MPCVD growth of NCD crystals on DND-seeded silicon substrates without CO<sub>2</sub> in the recipe. SEM images showing early stages of CVD diamond growth at (a) 3%, (b) 4%, and (c) 5% CH<sub>4</sub> after 15 min of growth at an average input power of 1500 W. (d) Raman signal from such NCD crystals.

If the NCD crystal densities are compared between silicon and sapphire substrates after 15 min of LA-MPCVD growth at 4% CH<sub>4</sub> without CO<sub>2</sub> (Figure 11a,b), it is found that there are 10 NCDs within a square area of 200 nm × 200 nm (Figure 11a) on Si and there are about 20 NCDs on sapphire substrate (Figure 11b). Hence, it may be inferred that sapphire substrates are more effective in growing the DND seeds. A similar trend is observed of the number of NCD crystals present on the sapphire substrate doubling in comparison to the silicon substrate after 15 min of LA-MPCVD growth at 5% CH<sub>4</sub> without CO<sub>2</sub> (Figure 11c,d).

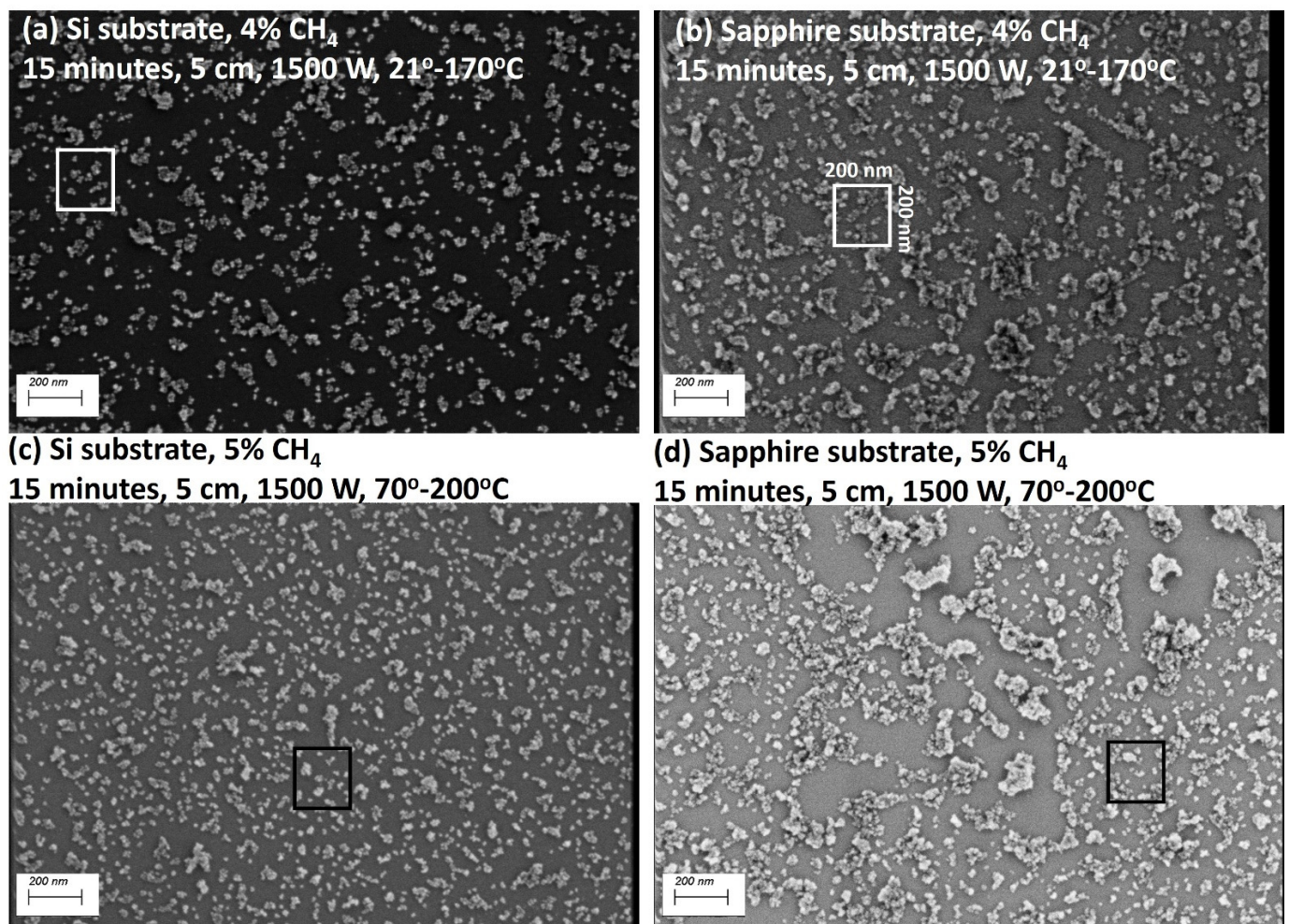


**Figure 11.** Comparison of LA-MPCVD growth (1500 W, 5 cm, 15 min) of NCD crystals on DND-seeded silicon and sapphire substrates without CO<sub>2</sub> in the recipe. NCD crystal (sample # LA200605-1) SEM 50 k $\times$  magnification images on (a) Si and (b) sapphire substrates at 4% CH<sub>4</sub>. NCDs (sample # LA200605-2) on (c) Si and (d) sapphire substrates at 5% CH<sub>4</sub>.

If we compare the NCD crystal densities on Si substrate with increasing CH<sub>4</sub> percentages, it is observed that there are more NCDs, 15 in number, within a square area of 200 nm  $\times$  200 nm (Figure 11c). Similarly, increasing the CH<sub>4</sub> percentage from 4% to 5% on the sapphire substrate also increases the NCD crystal densities from 20 to 30 NCDs present within a square area of 200 nm  $\times$  200 nm (Figure 11b,d) of the sapphire substrate after 15 min of LA-MPCVD growth. Thus, it can be concluded that the increasing methane percentages promoted LA-MPCVD growth of NCDs.

#### Effect of Deposition Time

The growth rate of linear antenna CVD is slower in comparison to conventional microwave plasma CVD growth of diamond crystals inside resonant cavity reactors. The typical growth rate for MPCVD is in the order of microns per hour [1,45], whereas inside LA-MPCVD, NCDs grow by 5–20 nm per hour [13,46], depending on the presence of CO<sub>2</sub> percentages in the recipe and also on the use of pulse mode, which favors higher growth rates. Hence, it is understood that a longer LA-MPCVD deposition time is required to fully cover the substrates with NCD films. The available literature reports only about the long deposition periods (mostly 8, 15, and 20 h of LA-MPCVD). There is little or no information about the growth of NCDs during the initial periods of LA-MPCVD, when the substrate temperature is not stabilized yet (Figure 1a) and is continuously increasing by heating



with plasma. Figure 1b is the cooling–heating cycle for the sample # LA200605-3, with 11 min of short LA-MPCVD deposition period, shown with a sudden rise in substrate temperature (from 88° to 270 °C) at 2800 W average input power and 5 cm stage-to-antenna distance. The experiment on sample # LA200605-1 started from room temperature with 4% CH<sub>4</sub> and the plasma heating lasted for 15 min, which continuously increased the substrate temperature up to 170 °C at 1500 W average input power and at 5 cm stage-to-antenna distance. Thereafter, the reactor was allowed to cool down below 140 °C (temperature safety-limit of the reactor) before it was re-opened to unload and reload the next set of 4 substrates. In this way, the starting temperature for the next set of samples, sample # LA200605-2, became 70 °C (not restarting from room temperature) and, again with 15 min of heating with 5% CH<sub>4</sub> in the hydrogen plasma, it could heat up to a slightly higher substrate temperature of 200 °C at 1500 W average input power and 5 cm stage-to-antenna distance. Again, the experiment was stopped, and the reactor was allowed to cool down to 88 °C (shown in Figure 1b and depending on the time one takes to load and unload samples) before restarting with sample # LA200605-3 for 11 min of plasma heating up to 270 °C, but at 2800 W power and 5 cm distance. The important point to be noted is that the heating rates were 9.9 °C/min for # LA200605-1, 8.6 °C/min for # LA200605-2, and 16.5 °C/min for # LA200605-3. The third LA-MPCVD heating rate was higher because of the very high input MW power level of 2800 W.

Figure 12a,c compare the diamond film growth behavior on silicon substrates after 15 min (1500 W) and 11 min (2800 W) of LA-MPCVD heating with 5% CH<sub>4</sub> in the hydrogen plasma recipe, respectively. There are almost equal numbers (about 45 diamond nanoparticles inside a 500 nm × 500 nm square) of whitish bright NCD particles scattered on the dark contrasting silicon substrate in both the images. Although there was a 4 min reduction in deposition time with concomitant increase in MW input power by 1300 W, Figure 12c shows somewhat sharper white spots of NCDs on Si, which may be due to its wider substrate temperature range of 88–270 °C. On the other hand, sapphire substrate has a higher number (approximately 70 diamond nanoparticles inside a 500 nm × 500 nm square) of NCDs scattered in Figure 12b. Moreover, there are also signs of nanodiamond agglomeration in Figure 12b. It may be concluded that sapphire substrate favored more lateral growth of DND seed crystals than silicon substrate. This may be attributed to a tendency for silicon to form carbide, which reduces the formation of diamond nanoparticles. The number of NCD particles present inside a 200 nm × 200 nm square area is about 20 in Figure 12d, for LA-MPCVD growth on sapphire substrate for 11 min with 5% CH<sub>4</sub> at 2800 W power and at 5 cm distance, which is almost equal in number to the NCD particle density found in Figure 11b for 15 min of LA-MPCVD with 4% CH<sub>4</sub> at 5 cm distance. The number of diamond nanoparticles was 30 in Figure 11d inside a 200 nm × 200 nm square area for 15 min of LA-MPCVD with 5% CH<sub>4</sub> at 5 cm distance. So, this decrease in NCD density number (30 to 20) with an identical LA-MPCVD recipe is mainly due to the decrease in deposition time from 15 to 11 min. It is important to note that although the MW input power was much higher (2800 W)—leading to higher substrate temperatures (88–270 °C)—it could not become effective in increasing the diamond nanoparticle density at shorter LA-MPCVD periods of 11 min.

Now, if the LA-MPCVD was allowed to proceed from 15 min to 30 min at 3% CH<sub>4</sub> in the process recipe without CO<sub>2</sub>, with simultaneous lowering of the stage from 5 to 6.5 cm distance away from the quartz tube antenna, it was found (inside 500 nm × 500 nm squares) that the NCD crystal sizes grow bigger in size with concomitant touch with each other to form some kind of agglomeration (Figure 13a,c) on silicon substrate surfaces. On the other hand, the NCD crystals are found already to be much bigger on sapphire substrates (Figure 13b,d) under identical LA-MPCVD processing conditions than on the silicon substrates, which is again due to the tendency of silicon to form carbide favorably over nanodiamond formation. There are about 15 NCD crystals/agglomerates inside 200 nm × 200 nm squares in Figure 13b, in comparison to approximately 10 NCD crystals/agglomerates inside 200 nm × 200 nm squares in Figure 13d. The NCD sizes vary

from as small as 25 nm individual crystals to as big an agglomeration size as 100 nm in Figure 13d, whereas the smallest NCD in Figure 13b is about 20 nm and the biggest agglomeration is found to be as big as 50–60 nm. Therefore, it may be concluded that longer deposition time allowed the NCDs to grow in the lateral direction, covering more of the underlying sapphire substrate gradually with time. The NCD crystals are found to be 40–45 nm in size (Figure 13c) on silicon substrate after 30 min of LACVD with 3% methane in hydrogen plasma, occasionally touching each other, whereas in Figure 13a (15 min) they remained isolated from each other with smaller (30–35 nm) diamond nanoparticle sizes.

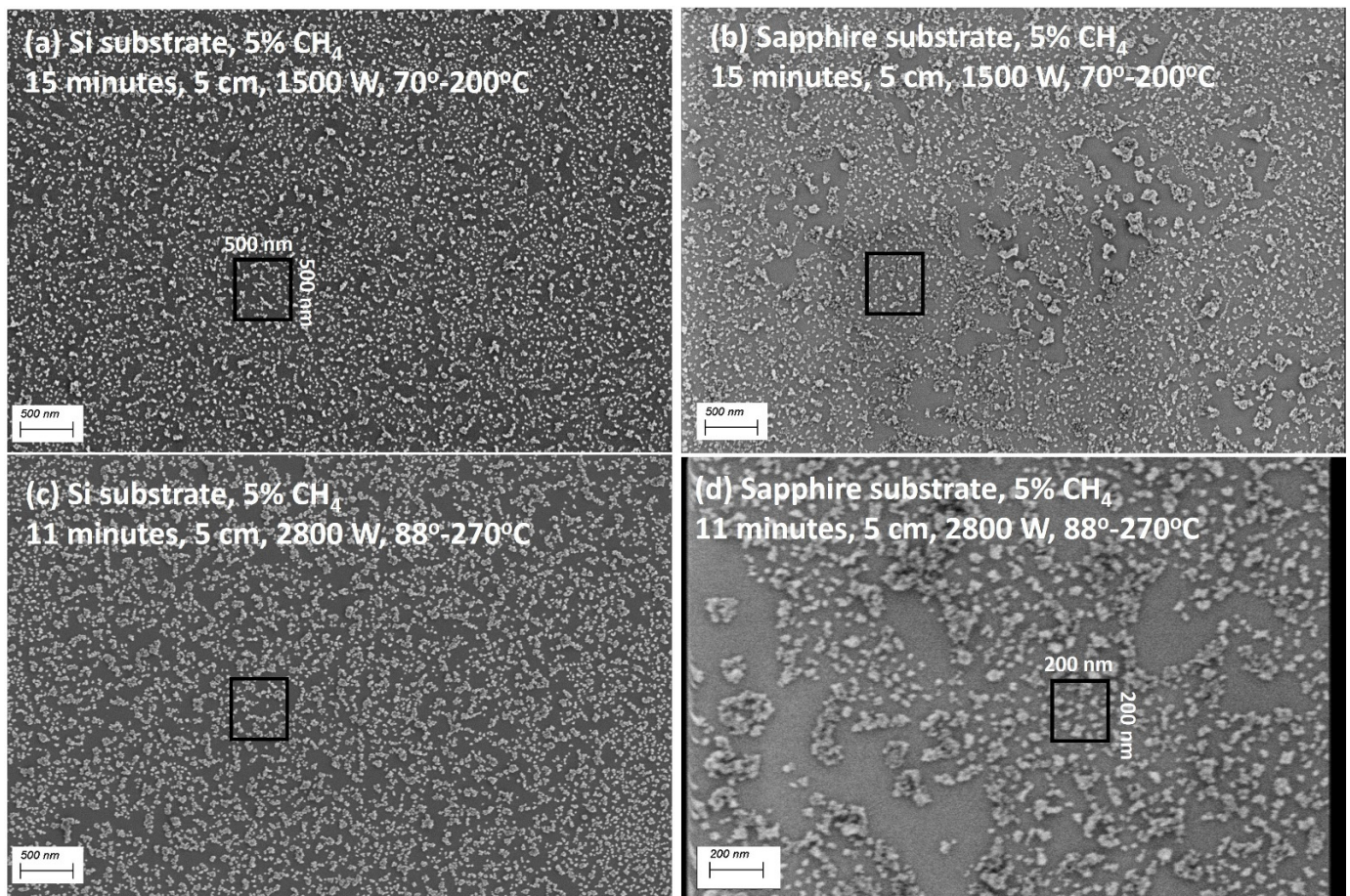


**Figure 12.** SEM images of LACVD-grown (1500 W, 5 cm) NCD crystals without CO<sub>2</sub> gas in the recipe, after 15 min on DND-seeded (a) silicon and (b) sapphire substrates and after 11 min on DND-seeded (c) silicon and (d) sapphire substrates.

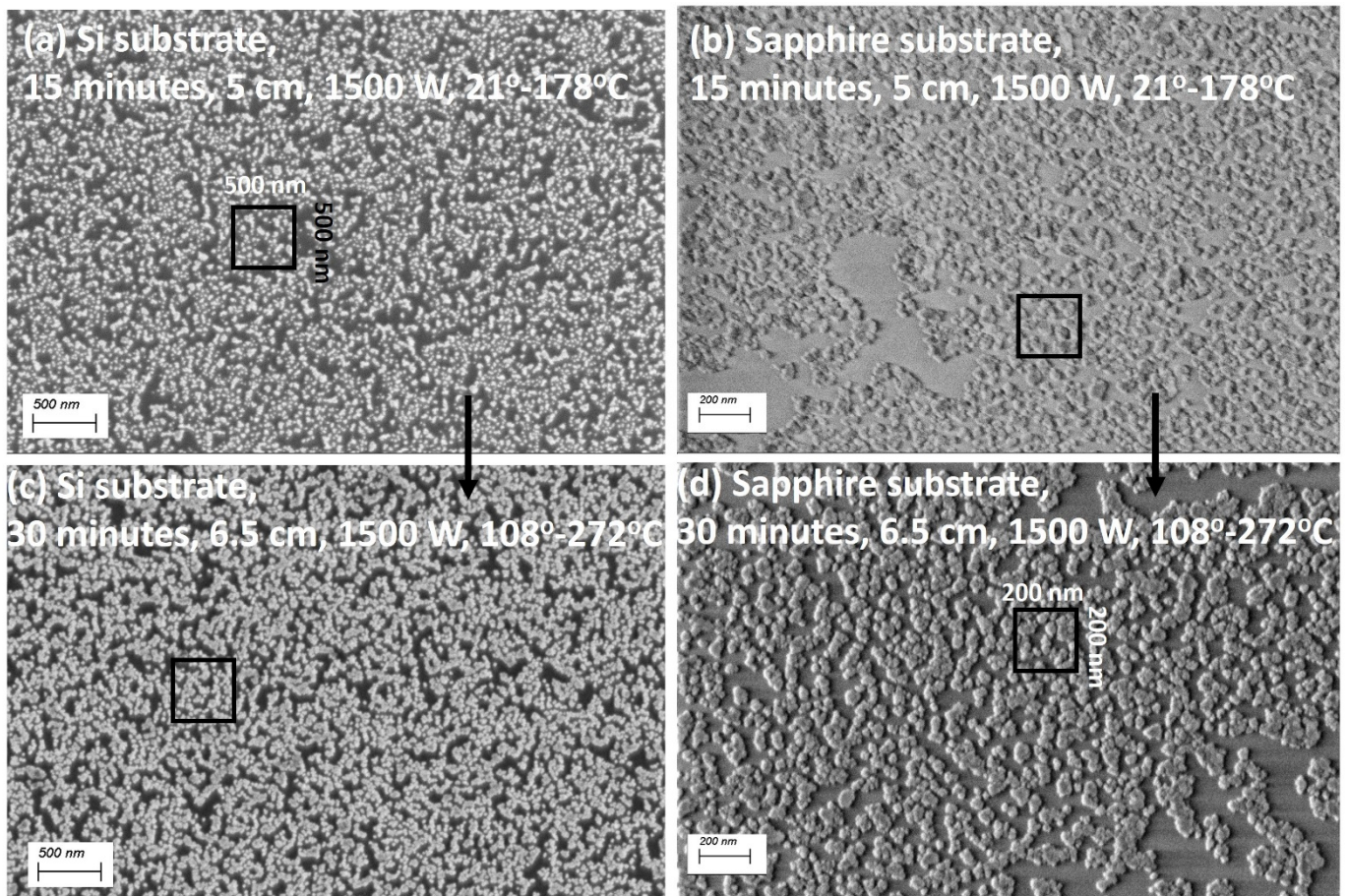


**Figure 13.** SEM images of LA-MPCVD-grown (1500 W) NCD crystals without CO<sub>2</sub> gas in the recipe, grown after 15 min on DND-seeded (a) silicon and (b) sapphire substrates at a 5 cm stage-to-antenna distance and grown after 30 min on DND-seeded (c) silicon and (d) sapphire substrates at a 6.5 cm stage-to-antenna distance.

#### 4. Conclusions

Early period growth of NCD crystals inside a LA-MPCVD reactor during the initial temperature rise of the substrates by microwave plasma heating, has been presented. It has been observed that:

- The substrate temperature keeps increasing during the first hours of LA-MPCVD and the NCD film remains discontinuous on the DND-seeded silicon and sapphire substrates.
- The short duration LA-MPCVD runs for 15 min were not effective in coalescing the NCD films, but they were found to be appropriate for coating CNTs with NCDs.
- The CNT/Si samples were found to be severely etched out under a H<sub>2</sub>/CH<sub>4</sub>/CO<sub>2</sub> = 89/5/6 plasma recipe—more than the EPD-treated CNT/Si substrates. Pre-treatment with electrophoretic diamond seeds helped in protecting the carbon nanotubes from plasma etching, as evident from their longer CNT lengths after 15 min of LA-MPCVD runs.
- Further prevention of plasma etching of the EPD-seeded CNT/Si substrate was observed without CO<sub>2</sub> gas in the LA-MPCVD process recipe, with evidence of 25 μm long CNTs present even after 30 min of LA-MPCVD runs.
- DND-seeded sapphire substrates were found to favor the formation of bigger and denser NCD particles than the silicon substrates. Moreover, the Raman signals were also found to be relatively better from sapphire substrates (FWHM of sp<sup>3</sup> = 15 cm<sup>-1</sup>) than from the NCDs on silicon substrate, under identical LA-MPCVD parameters.

- (f) Lowering of the input microwave power level from 1500 to 1100 W in continuous wave mode favored the formation of connected NCDs.
- (g) On the other hand, pulse mode LA-MPCVD experiments were also found to help in improving NCD crystal formation with bigger grain sizes (40–90 nm on Si) and more effective surface coverage of the substrates.
- (h) Increasing the stage-to-antenna distance from 5 cm to 6.5 cm promoted the formation of secondary nucleation sites. Re-nucleation at longer substrate-to-quartz-tube distances, along with a longer deposition time of 2 h, are found to be essential in growing continuous NCD films.
- (i) The effect of increasing CH<sub>4</sub> percentages in the process recipe was to supply more carbon atoms necessary for increasing the densities of diamond nanoparticles on DND-seeded substrates.
- (j) Deposition time is the most important factor for NCD growth during the early stages of LA-MPCVD. Even a higher input power of 2800 W (and therefore higher temperatures) could not significantly affect the NCD crystal sizes within short periods of time.
- (k) It was necessary to run the LA-MPCVD experiments for long enough (2 h) to achieve a flat stable substrate temperature (263 °C).

**Author Contributions:** A.K.M.: conceptualization, methodology, formal analysis, investigation, resources, data curation, writing—original draft preparation, writing—review and editing, visualization; W.-C.S.: conceptualization, methodology, formal analysis, investigation, resources, data curation, writing—review and editing, visualization; P.P.: conceptualization, methodology, formal analysis, investigation, resources, data curation, writing—review and editing, visualization; K.H.: conceptualization, validation, writing—review and editing, visualization, supervision, project administration, funding acquisition. All authors have read and agreed to the published version of the manuscript.

**Funding:** This work was financially supported by the Methusalem NANO network and the Research Foundation—Flanders (FWO) via project G0D4920N. AKM acknowledges FWO for his Postdoctoral Fellowship with grant no. 12X2919N.

**Institutional Review Board Statement:** Not applicable.

**Informed Consent Statement:** Not applicable.

**Data Availability Statement:** Data are contained within the article.

**Acknowledgments:** All data generated or analyzed during this study are included in this published article. The datasets generated during and/or analyzed during the current study are available from the corresponding author on reasonable request.

**Conflicts of Interest:** The authors declare that they have no known competing financial interests or personal relationships that could have appeared to influence the work reported in this paper.

## References

1. Grotjohn, T.A.; Asmussen, J. Microwave Plasma-Assisted Diamond Film Deposition. In *Diamond Films Handbook*; Asmussen, J., Reinhard, D.K., Eds.; Marcel Dekker, Inc.: New York, NY, USA, 2002; Chapter 7.
2. Das, D.; Singh, R.N. A review of nucleation, growth and low temperature synthesis of diamond thin films. *Int. Mater. Rev.* **2007**, *52*, 29–64. [[CrossRef](#)]
3. Piazza, F.; Morell, G. Synthesis of diamond at sub 300 °C substrate temperature. *Diam. Relat. Mater.* **2007**, *16*, 1950–1957. [[CrossRef](#)]
4. Ihara, M.; Maeno, H.; Miyamoto, K.; Komiyama, H. Low-temperature deposition of diamond in a temperature range from 70 °C to 700 °C. *Diam. Relat. Mater.* **1992**, *1*, 187–190. [[CrossRef](#)]
5. Potocky, S.; Kromka, A.; Potmesil, J.; Remes, Z.; Polackova, Z.; Vanecek, M. Growth of nanocrystalline diamond films deposited by microwave plasma CVD system at low substrate temperatures. *Phys. Status Solidi* **2006**, *203*, 3011–3015. [[CrossRef](#)]
6. Gueroudji, L.; Hwang, N.M. Thermodynamic limits for the substrate temperature in the CVD diamond process. *Diam. Relat. Mater.* **2000**, *9*, 205–211. [[CrossRef](#)]
7. Gu, J.; Chen, Z.; Li, R.; Zhao, X.; Das, C.; Sahnuganathan, V.; Sudijono, J.; Lin, M.; Loh, K.P. Nanocrystalline diamond film grown by pulsed linear antenna microwave CVD. *Diam. Relat. Mater.* **2021**, *119*, 108576. [[CrossRef](#)]
8. Tsugawa, K.; Ishihara, M.; Kim, J.; Hasegawa, M.; Koga, Y. Large-Area and Low-Temperature Nanodiamond Coating by Microwave Plasma Chemical Vapor Deposition. *New Diam. Front. Carbon Technol.* **2006**, *16*, 337–346.

9. Marton, M.; Vojs, M.; Michniak, P.; Behúl, M.; Rehacek, V.; Pifko, M.; Stehlík, S.; Kromka, A. New chemical pathway for large-area deposition of doped diamond films by linear antenna microwave plasma chemical vapor deposition. *Diam. Relat. Mater.* **2022**, *126*, 109111. [[CrossRef](#)]
10. Kromka, A.; Babchenko, O.; Izak, T.; Hruska, K.; Rezek, B. Linear antenna microwave plasma CVD deposition of diamond films over large areas. *Vacuum* **2012**, *86*, 776–779. [[CrossRef](#)]
11. Fendrych, F.; Taylor, A.; Peksa, L.; Kratochvilova, I.; Vlcek, J.; Rezacova, V.; Petrak, V.; Kluibler, Z.; Fekete, L.; Liehr, M.; et al. Growth and characterization of nanodiamond layers prepared using the plasma-enhanced linear antennas microwave CVD system. *J. Phys. D Appl. Phys.* **2010**, *43*, 374018. [[CrossRef](#)]
12. Potocký, Š.; Babchenko, O.; Hruška, K.; Kromka, A. Linear antenna microwave plasma CVD diamond deposition at the edge of no-growth region of C-H-O ternary diagram. *Phys. Status Solidi* **2012**, *249*, 2612–2615. [[CrossRef](#)]
13. Taylor, A.; Fendrych, F.; Fekete, L.; Vlček, J.; Řezáčová, V.; Petrák, V.; Krucký, J.; Nesládek, M.; Liehr, M. Novel high frequency pulsed MW-linear antenna plasma-chemistry: Routes towards large area, low pressure nanodiamond growth. *Diam. Relat. Mater.* **2011**, *20*, 613–615. [[CrossRef](#)]
14. Izak, T.; Babchenko, O.; Varga, M.; Potocky, S.; Kromka, A. Low temperature diamond growth by linear antenna plasma CVD over large area. *Phys. Status Solidi* **2012**, *249*, 2600–2603. [[CrossRef](#)]
15. Drijkoningen, S.; Pobedinskas, P.; Korneychuk, S.; Momot, A.; Balasubramaniam, Y.; Van Bael, M.K.; Turner, S.; Verbeeck, J.; Nesla, M.; Haenen, K. On the Origin of Diamond Plates Deposited at Low Temperature. *Cryst. Growth Des.* **2017**, *17*, 4306–4314. [[CrossRef](#)]
16. Mistrik, J.; Janicek, P.; Taylor, A.; Fendrych, F.; Fekete, L.; Jager, A.; Nesladek, M. Spectroscopic ellipsometry characterization of nano-crystalline diamond films prepared at various substrate temperatures and pulsed plasma frequencies using microwave plasma enhanced chemical vapor deposition apparatus with linear antenna delivery. *Thin Solid Films* **2014**, *571*, 230–237. [[CrossRef](#)]
17. Tsugawa, K.; Ishihara, M.; Kim, J.; Koga, Y.; Hasegawa, M. Nanocrystalline diamond film growth on plastic substrates at temperatures below 100 °C from low-temperature plasma. *Phys. Rev. B* **2010**, *82*, 125460. [[CrossRef](#)]
18. Neykova, N.; Kozak, H.; Ledinsky, M.; Kromka, A. Novel plasma treatment in linear antenna microwave PECVD system. *Vacuum* **2012**, *86*, 603–607. [[CrossRef](#)]
19. Bénédic, F.; Belmahi, M.; Easwarakhanthan, T.; Alnot, P. In situ optical characterization during MPACVD diamond film growth on silicon substrates using a bichromatic infrared pyrometer under oblique incidence. *J. Phys. D Appl. Phys.* **2001**, *34*, 1048. [[CrossRef](#)]
20. Gracio, J.J.; Fan, Q.H.; Madaleno, J.C. Diamond growth by chemical vapour deposition. *J. Phys. D Appl. Phys.* **2010**, *43*, 374017. [[CrossRef](#)]
21. Kromka, A.; Potocký, Š.; Čermák, J.; Rezek, B.; Potměšil, J.; Zemek, J.; Vaněček, M. Early stage of diamond growth at low temperature. *Diam. Relat. Mater.* **2008**, *17*, 1252–1255. [[CrossRef](#)]
22. Babchenko, O.; Potocký, Š.; Ižák, T.; Hruška, K.; Brykhar, Z.; Kromka, A. Influence of surface wave plasma deposition conditions on diamond growth regime. *Surf. Coat. Technol.* **2015**, *271*, 74–79. [[CrossRef](#)]
23. Bai, T.; Wang, Y.; Feygelson, T.I.; Tadjer, M.J.; Hobart, K.D.; Hines, N.J.; Yates, L.; Graham, S.; Anaya, J.; Kuball, M.; et al. Diamond Seed Size and the Impact on Chemical Vapor Deposition Diamond Thin Film Properties. *ECS J. Solid State Sci. Technol.* **2020**, *9*, 053002. [[CrossRef](#)]
24. Pobedinskas, P.; Janssens, S.D.; Hernando, J.; Wagner, P.; Nesládek, M.; Haenen, K. Selective seeding and growth of nanocrystalline CVD diamond on non-diamond substrates. *MRS Proc.* **2011**, *1339*, 1–6. [[CrossRef](#)]
25. Pobedinskas, P.; Degutis, G.; Dexters, W.; Janssen, W.; Janssens, S.D.; Conings, B.; Ruttens, B.; D'Haen, J.; Boyen, H.-G.; Hardy, A.; et al. Surface plasma pretreatment for enhanced diamond nucleation on AlN. *Appl. Phys. Lett.* **2013**, *102*, 201609. [[CrossRef](#)]
26. Rotter, S.Z.; Madaleno, J.C. Diamond CVD by a Combined Plasma Pretreatment and Seeding Procedure. *Chem. Vap. Depos.* **2009**, *15*, 209–216. [[CrossRef](#)]
27. Tsugawa, K.; Ishihara, M.; Kim, J.; Koga, Y.; Hasegawa, M. Nucleation Enhancement of Nanocrystalline Diamond Growth at Low Substrate Temperatures by Adamantane Seeding. *J. Phys. Chem. C* **2010**, *114*, 3822–3824. [[CrossRef](#)]
28. Arnault, J.C.; Demuynck, L.; Speisser, C.; Normand, F.L. Mechanisms of CVD diamond nucleation and growth on mechanically scratched Si(100) surfaces. *Eur. Phys. J. B Condens. Matter Complex Syst.* **1999**, *11*, 327–343. [[CrossRef](#)]
29. Buijnsters, J.; Vázquez, L.; ter Meulen, J. Substrate pre-treatment by ultrasonication with diamond powder mixtures for nucleation enhancement in diamond film growth. *Diam. Relat. Mater.* **2009**, *18*, 1239–1246. [[CrossRef](#)]
30. Shenderova, O.; Hens, S.; McGuire, G. Seeding slurries based on detonation nanodiamond in DMSO. *Diam. Relat. Mater.* **2010**, *19*, 260–267. [[CrossRef](#)]
31. Domonkos, M.; Ižák, T.; Varga, M.; Potocký, Š.; Demo, P.; Kromka, A. Diamond nucleation and growth on horizontally and vertically aligned Si substrates at low pressure in a linear antenna microwave plasma system. *Diam. Relat. Mater.* **2018**, *82*, 41–49. [[CrossRef](#)]
32. Affoune, A.M.; Prasad, B.L.V.; Sato, H.; Enoki, T. Electrophoretic Deposition of Nanosized Diamond Particles. *Langmuir* **2001**, *17*, 547–551. [[CrossRef](#)]
33. Tsubota, T.; Ida, S.; Okada, N.; Nagata, M.; Matsumoto, Y.; Yatsushiro, N. CVD diamond coating on WC–Co cutting tool using ECR MPCVD apparatus via electrophoretic seeding pretreatment. *Surf. Coat. Technol.* **2003**, *169–170*, 262–265. [[CrossRef](#)]

34. Chang, T.-H.; Panda, K.; Panigrahi, B.K.; Lou, S.-C.; Chen, C.; Chan, H.-C.; Lin, I.-N.; Tai, N.-H. Electrophoresis of Nanodiamond on the Growth of Ultrananocrystalline Diamond Films on Silicon Nanowires and the Enhancement of the Electron Field Emission Properties. *J. Phys. Chem. C* **2012**, *116*, 19867–19876. [[CrossRef](#)]
35. Smith, E.; Piracha, A.; Field, D.; Pomeroy, J.; Mackenzie, G.; Abdallah, Z.; Massabuau, F.-P.; Hinz, A.; Wallis, D.; Oliver, R.; et al. Mixed-size diamond seeding for low-thermal-barrier growth of CVD diamond onto GaN and AlN. *Carbon* **2020**, *167*, 620–626. [[CrossRef](#)]
36. Potocký, Š.; Čada, M.; Babchenko, O.; Ižák, T.; Davydova, M.; Kromka, A. Perspectives of linear antenna microwave system for growth of various carbon nano-forms and its plasma study. *Phys. Status Solidi* **2013**, *250*, 2723–2726. [[CrossRef](#)]
37. Potocký, Š.; Babchenko, O.; Davydova, M.; Izak, T.; Čada, M.; Kromka, A. Growth of carbon allotropes and plasma characterization in linear antenna microwave plasma CVD system. *Jpn. J. Appl. Phys.* **2014**, *53*, 05FP04. [[CrossRef](#)]
38. Zou, Y.; May, P.W.; Vieira, S.M.C.; Fox, N.A. Field Emission from Diamond-Coated Multiwalled Carbon Nanotube “Teepee” Structures. *J. Appl. Phys.* **2012**, *112*, 044903. [[CrossRef](#)]
39. Chang, T.; Kunuku, S.; Hong, Y.; Leou, K.; Yew, T.; Tai, N.; Lin, I. Enhancement of the Stability of Electron Field Emission Behavior and the Related Microplasma Devices of Carbon Nanotubes by Coating Diamond Films. *ACS Appl. Mater. Interfaces* **2014**, *6*, 11589–11597. [[CrossRef](#)]
40. Fiori, A.; Orlanducci, S.; Sessa, V.; Tamburri, E.; Toschi, F.; Terranova, M.L.; Ciorba, A.; Rossi, M.; Lucci, M.; Barnard, A.S. Hybrid Carbon Nanotube/Nanodiamond Structures as Electron Emitters for Cold Cathodes. *J. Nanosci. Nanotechnol.* **2008**, *8*, 1989–1993. [[CrossRef](#)]
41. Williams, O.A.; Douheret, O.; Daenen, M.; Haenen, K.; Osawa, E.; Takahashi, M. Enhanced diamond nucleation on monodispersed nanocrystalline diamond. *Chem. Phys. Lett.* **2007**, *445*, 255–258. [[CrossRef](#)]
42. Hu, L.; Guo, Y.; Du, S.; Tian, S.; Li, J.; Gu, C. Probing trans-polyacetylene segments in a diamond film by tip-enhanced Raman spectroscopy. *Diam. Relat. Mater.* **2021**, *116*, 108415. [[CrossRef](#)]
43. Tsugawa, K.; Kawaki, S.; Ishihara, M.; Kim, J.; Koga, Y.; Sakakita, H.; Koguchi, H.; Hasegawa, M. Nanocrystalline diamond growth in a surface-wave plasma. *Diam. Relat. Mater.* **2011**, *20*, 833–838. [[CrossRef](#)]
44. Taylor, A.; Ashcheulov, P.; Čada, M.; Fekete, L.; Hubík, P.; Klimša, L.; Olejníček, J.; Remeš, Z.; Jirka, I.; Janíček, P.; et al. Effect of plasma composition on nanocrystalline diamond layers deposited by a microwave linear antenna plasma-enhanced chemical vapour deposition system. *Phys. Status Solidi* **2015**, *212*, 2418–2423. [[CrossRef](#)]
45. Mallik, A.K.; Bysakh, S.; Sreemany, M.; Roy, S.; Ghosh, J.; Roy, S.; Mendes, J.C.; Gracio, J.; Datta, S. Property mapping of pol-ycrystalline diamond coatings over large area. *J. Adv. Ceram.* **2014**, *3*, 56–70. [[CrossRef](#)]
46. Mallik, A.K.; Lloret, F.; Gutierrez, M.; Rouzbahani, R.; Pobedinskas, P.; Shih, W.C.; Haenen, K. Deposition and Characterisation of a Diamond/Ti/Diamond Multilayer Structure. *Coatings* **2023**, *13*, 1914. [[CrossRef](#)]

**Disclaimer/Publisher’s Note:** The statements, opinions and data contained in all publications are solely those of the individual author(s) and contributor(s) and not of MDPI and/or the editor(s). MDPI and/or the editor(s) disclaim responsibility for any injury to people or property resulting from any ideas, methods, instructions or products referred to in the content.